Application of Wrapping Cams in an Unpowered, Upper-Limb Assistive Device

A Thesis

Presented in Partial Fulfillment of the Requirements for the

Degree of Master of Science

with a

Major in Mechanical Engineering

in the

College of Graduate Studies

University of Idaho

by

Jeremiah S. Schroeder

Major Professor: Joel C. Perry, Ph.D.

Committee Members: Eric T. Wolbrecht, Ph.D.; Edwin M. Odom, Ph.D.

Department Administrator: Steven W. Beyerlein, Ph.D.

December 2016

Authorization to Submit Thesis

This thesis of Jeremiah Schroeder, submitted for the degree of Master of Science with a Major in Mechanical Engineering and titled "Application of Wrapping Cams in an Unpowered, Upper-Limb Assistive Device," has been reviewed in final form. Permission, as indicated by the signatures and dates below, is now granted to submit final copies to the College of Graduate Studies for approval.

Major Professor: _____ Date: _____
Joel C. Perry, Ph.D.

Committee Members: _____ Date: _____
Eric T. Wolbrecht, Ph.D.

_____ Date: _____
Edwin M. Odom, Ph.D.

Department Administrator: _____ Date: _____
Steven W. Beyerlein, Ph.D.

Abstract

This thesis presents the development of two novel gravity balance mechanisms for use in spring-based, wearable arm support devices for stroke rehabilitation. The first mechanism, called the series wrapping cam, uses a cam coupled to shoulder elevation to drive the rotation of a second cam, which in turn stretches a spring. The first cam, called the drive cam, gives the second cam, called the spring cam, a high mechanical advantage when the arm is horizontal. This allows a low initial spring tension and spring cam radius. This mechanical advantage decreases as the arm is lowered, optimally utilizing the available rotation of the cams. A two degree of freedom prototype arm support was constructed to demonstrate the application of the series wrapping cam as an arm support mechanism. The prototype features a lightweight, compact spring made from latex tubing. A series cam mechanism was synthesized which uses this spring's full linear range of motion, minimizing the size of the spring. Vectran synthetic fiber rope was used as the wrapping element in the cams due to its tolerance to bending. The series wrapping cam prototype creates the correct general torque profile for an arm support, but the prototype does not respond appropriately to elbow flexion. The second mechanism was designed to couple elbow flexion with a support mechanism on the upper arm. It uses wrapping cams to apply the simultaneous displacement method for energy free adjustment of gravity balancers. A three degree of freedom prototype was constructed to demonstrate this mechanism. The prototype is able to support the upper arm, adjust the upper-arm support in response to elbow flexion/extension, and support elbow flexion using only one spring mechanism placed alongside the upper arm. Of the 4 anthropomorphic degrees of freedom from the glenohumeral joint to the elbow, the prototype excludes shoulder internal/external rotation. Future improvement and applications of the mechanisms are discussed.

Acknowledgements

I would like to acknowledge my major professor, Dr. Joel Perry, without whom this work would not have been possible. Thank you for generously providing funding through your own startup funds for both research expenses and my stipends. Thank you also for your patient guidance and advice throughout this project as well as your editorial help in writing my thesis.

Thanks to my committee members, Dr. Eric Wolbrecht and Dr. Edwin Odom for taking the time to review my thesis and take part in its defense.

I would also like to thank those that helped me complete the prototypes presented in this thesis. I especially appreciate our machine shop manager, Russ Porter, who provided immeasurable help through his patient advice on both design and machining technique. I would also like to thank James Hunter of the WSU Instrumentation shop and James Mader of the UI Facilities Machine Shop for machining my most difficult parts. Also, thank you, James Mader, for sacrificing part of your weekends to keep our shop functioning in Russ's absence.

I must also acknowledge the countless friends and family members that have supported, encouraged, and prayed for me over the last two years. Thanks to my colleagues Kyle Morse and Stephen Goodwin for their guidance and input on my research. Thanks to my brothers Jacob and Joshua for their inspiring examples of hard-working, godly men. Finally, thanks especially to my parents, Philip and Lura for their endless love, encouragement, and generosity.

Table of Contents

List of Figures

List of Tables

1 Introduction

1.1 Background

Sixty-five percent of people who suffer a stroke are unable to incorporate their affected hand into activities of daily living (ADL's) six months after the stroke [1]. With approximately 795,000 people in the United States suffering a stroke each year [2], this creates a significant demand for upper-limb rehabilitative technology. New assistive devices for in-home use could improve a person's independence and functional usage of the affected limb. According to Han et. al. [3], stroke patients can continue to improve functional use of their affected limb after the cessation of therapy, but only if they reach a certain threshold of "spontaneous arm use [3]." If the ability of their affected limb is below this threshold, they will prefer to use compensatory strategies over using their affected limb. Use of the affected limb may be forced by restraining the unaffected limb, a technique known as constraint-induced movement therapy. This therapy has been shown to improve the functionality of the affected limb [4]. However, if an assistive device encouraged the use of their affected limb in ADL's, it could effectively help the user reach this threshold of spontaneous arm use, allowing continued improvement in functionality after the cessation of therapy, without constraining the unaffected limb.

Passive arm supports are assistive devices that use springs to store and return an arm's gravitational energy as its elevation changes, making the arm feel lighter or weightless. A wearable arm support could encourage spontaneous arm use among victims of stroke (and other neuromuscular related disabilities) in two ways. First, the affected side is often weak, making it difficult to raise the arm [5]. Second, an abnormal synergy between shoulder abduction and elbow flexion exists, which reduces the arm's range of motion by making it difficult to extend

the elbow when the arm is raised [6]. Supporting the weight of an affected arm diminishes this undesired elbow flexion giving the arm a greater workspace [7] as shown in Figure 1.

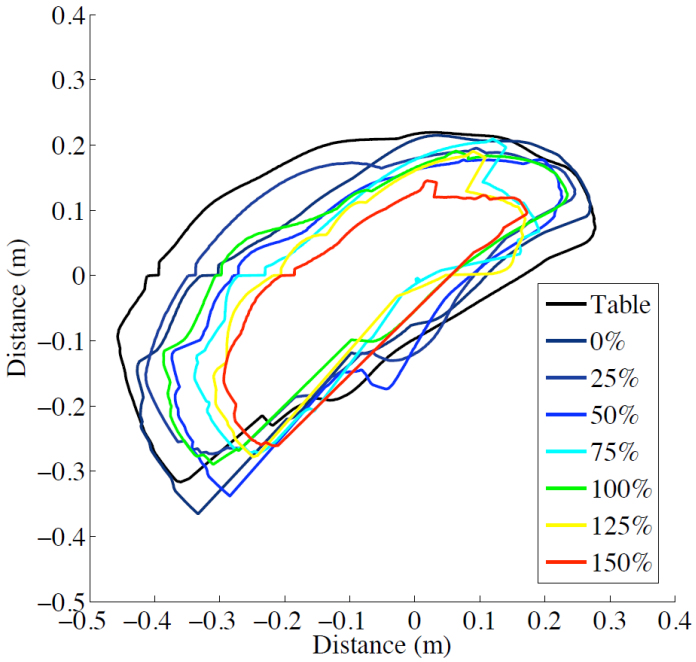

Figure 1. A plot of arm workspace for various levels of arm support taken from [7]. The arm was supported using a haptic robot as the person attempted to reach as far as possible in a circular movement in the horizontal plane. Different colored loops represent different percentages of the arm's weight that the subject was required to lift. That is, 0% is when the arm is fully supported and 150% is when the robot pulls the arm downward with a force equal to half the arm's weight.

1.2 The Traditional Gravity Balancing Mechanism

Passive arm supports are an application of gravity balancing mechanisms. The goal of a gravity balance mechanism is to statically balance the mechanism against gravitational forces regardless of the position it is placed in. This is equivalent to storing any change in gravitational potential energy as some other form of potential energy, typically elastic potential energy. A simple mechanism, shown in Figure 2, exists for balancing a weighted link, such as a human arm. In its simplest form, this mechanism consists of a "zero-length spring" attached to the supported link on one end and to a fixed point directly above the link's rotation axis on the other end. A zero length spring has a linear force-length relationship which, if extrapolated beyond the physical range of motion of the spring, has zero force when the length is zero. No

steel coil spring can physically relax to have zero length, so some initial tension must exist in the spring when its coils are closed [8].

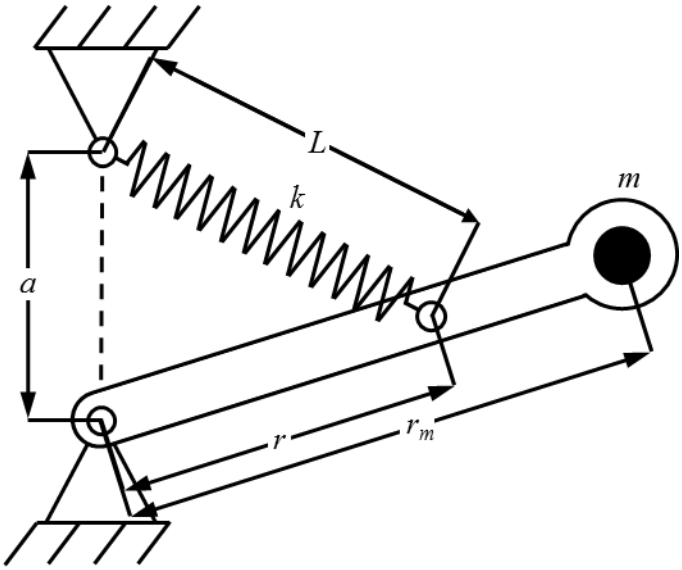

Figure 2. A traditional gravity balance mechanism [8].

This mechanism produces a torque about the axis of rotation which varies with the cosine of the angle of the link from the horizontal. Equivalently, it can be considered to apply a constant vertical force at some point on the link. This is demonstrated in Figure 3, which shows the force applied by the spring broken into a vertical component, and a component collinear with the link, which produces no supporting moment. The link can then be balanced such that the torque produced by the spring matches the torque produced by the weight of the link in all locations. To accomplish this, the following requirement must be met:

$$ark = r_m W \ , \tag{1}$$

where a is the distance between the rotation axis and the attachment point of the spring to the base; r is the distance between the rotation axis and the attachment point of the spring to the link; k is the spring rate; r_m is the distance from the rotation axis to the center of mass of the link; and W is the weight of the link [8].

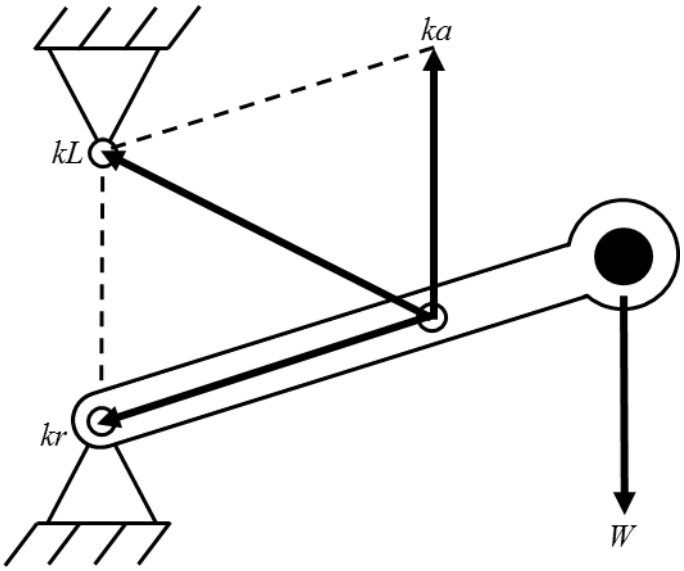

Figure 3. Decomposition of the spring force into vertical and unsupporting components [8]. The use of a zero length spring makes the force form the spring proportional to the length of the spring. Thus, the two components shown are proportional to the dimensions *a* and *r*, and remain constant.

This mechanism can be extended to support subsequent links. This is commonly accomplished by replacing all but the most distal supported link with parallelogram linkages, as shown in Figure 4. This provides any subsequent link with an anchor point that remains directly above the rotation axis for attachment of a support spring. This arrangement has been commonly applied in balanced desk lamps for decades [8].

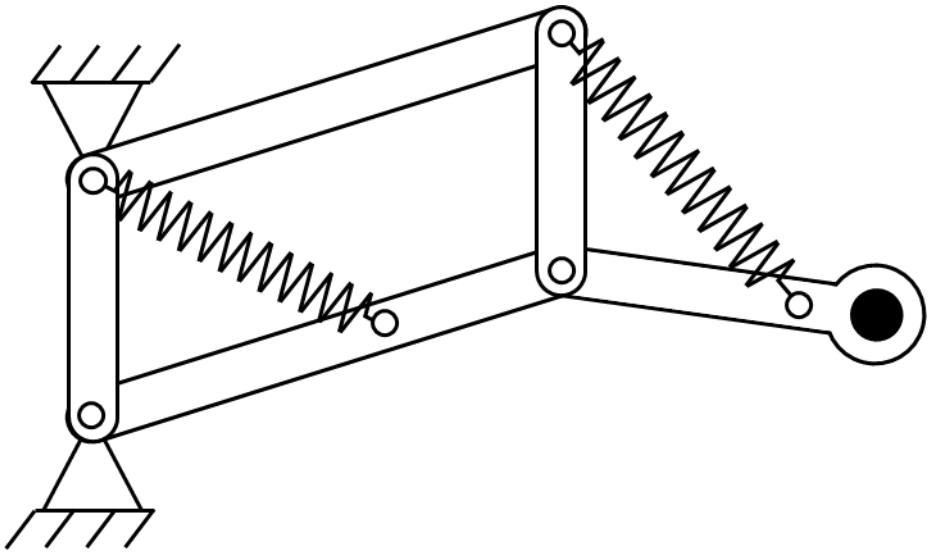

Figure 4. A two degree of freedom, planar, gravity balanced mechanism [8].

1.3 Existing Arm Support Devices

Variations on this concept have been applied in a variety of arm support devices. Many of these devices utilize an end effector configuration. This means that the linkages of the device do not mimic the kinematics of the human arm and the device only connects to the arm at one point. These usually balance both the upper arm and forearm by applying a constant vertical force to their "combined center of mass [9]." The SaeboMAS [10], Jaeco Elevating MAS [11], and Armon Edero [12] are table-mounted devices that utilize this principle.

Figure 5. The Darwing chair mounted arm support manufactured by Focal Meditech [13].

Various end-effector arm supports have been developed to mount to a wheelchair, including the Jaeco MAS and Armon Edero mentioned above. Additional devices include the Dynamic Arm Support (DAS) [14], the Armon [15], the Gowing [16], and the Darwing [13]. The Jaeco MAS, Armon Edero, Darwing, and the DAS all use a series of vertical joints to allow the end effector to move freely in the horizontal plane which does not allow these devices to remain close to the user's body. The Armon and the Gowing however use a planar two degree-of-freedom (DOF) mechanism with two support springs. The base of this mechanism is placed behind the user's arm with a link extending above their arm to the end-effector. This design

keeps most of the device close to and behind the user where it is less visible to those facing the user as well as less likely to interfere with objects in the arm's workspace. The Darwing, shown in Figure 5, uses two support mechanism placed in series to balance the upper arm and forearm independently. The base of the mechanism is placed just behind the user's shoulder so that the first supported link extends underneath the upper arm. The forearm is supported with a low profile cuff which is gravity balanced by a mechanism housed in the link under the upper arm. The Darwing remains somewhat close to the user's arm, but it is not strictly an exoskeleton.

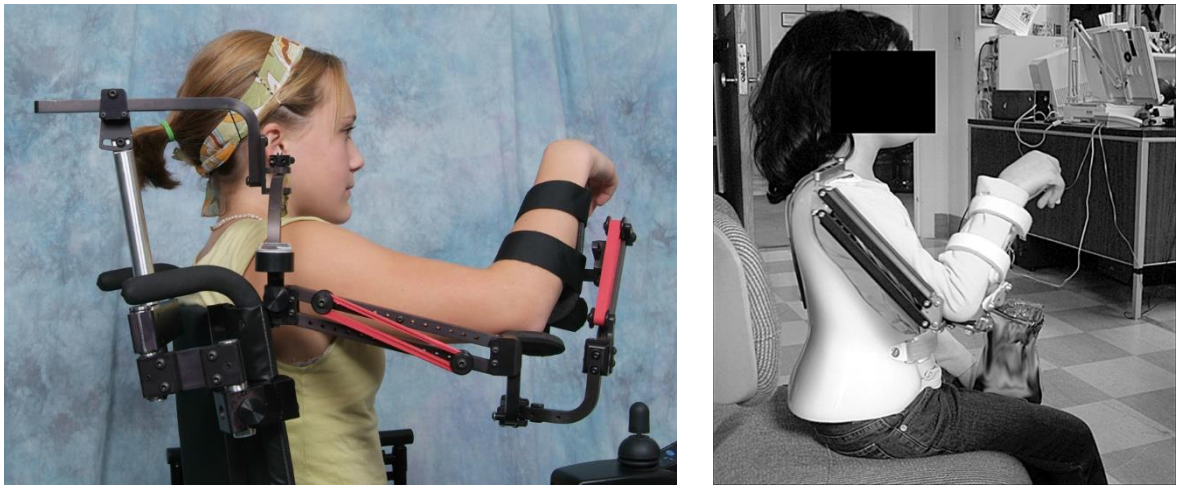

(a) (b)

Figure 6. The Wilmington Robotic Exoskeleton (WREX). (a) The chair mounted configuration of the marketed by Jaeco Orthopedics [17]. (b) One of the wearable prototypes tested by [18].

The Wilmington Robotic Exoskeleton (WREX), shown in Figure 6, is a four-DOF passive arm support exoskeleton. It features a gravity-balanced parallelogram linkage placed parallel to the upper arm and a second gravity balanced link placed parallel to the forearm. Vertical joints are placed above the shoulder and under the elbow with links wrapping around these arms joints to the horizontal joints of the two supported links. The WREX was tested with five children with arthrogryposis in both wearable and chair mounted configurations [18]. Since the study, a chair mounted version of the WREX has been commercially available through

Jaeco Orthopedics [19]. Wearable applications of the WREX, however, have not been widely used.

1.4 Opportunities for Improvement

For wearable arm support devices to become more widely used, some disincentives to their use must be addressed. The primary focus of this research was reducing the size, weight, and visibility of the device. A low profile device is valuable, as potential users desire to appear as normal as possible. Likewise a bulky design is more likely to interfere with the environment. In a state of the art review of arms supports, Dunning and Herder [20] evaluated the device profile as the volume of the device further than 20 mm from the body. Reducing the weight of a device decreases the discomfort of supporting the device at its attachment to the body. Likewise, reducing the inertia of any moving parts will reduce the user's perception of the device and allow them to move more freely. Comfortable and unrestrictive attachment of the device to the user's torso and arm is also a critical design challenge but was not considered in detail in this research.

The WREX, specifically, could be improved in a number of ways. The support mechanism next to the forearm dramatically increases the visibility and volume of the device. Because this support mechanism requires a base link that remains vertical, the elbow joint must wrap underneath the elbow to a vertical revolute joint, then wrap back up the elbow to the forearm link. If the support mechanism for the forearm could be placed in a more proximal link, as it is in the Darwing, the visibility, and possibly the inertia, of the device could be dramatically reduced. The WREX could be improved further if a more compact and concealable support mechanism could be implemented.

1.5 Wrapping Cams

1.5.1 Wrapping Cam Background

A specific type of mechanism, called a wrapping cam, was used extensively in this research. A traditional plate cam consists of a plate with a non-constant radius. An output link, called a follower, rests directly on and slides or rolls across the perimeter of the cam as it rotates. Thus, the follower will follow a path specified by the geometry of the cam. A wrapping cam, however, uses a flexible follower such as a rope, band, belt, or chain that wraps around its perimeter rather than pressing into and sliding across the perimeter. A wrapping cam can then be designed to cause the pulley about which the other end of the rope wraps to rotate according to an arbitrary function. A wrapping cam may also be designed to exert a specified force or torque if attached in some manner to a weight or spring [21]. This ability to specify an arbitrary force profile makes the wrapping cam a possible alternative to the traditional gravity balancing mechanism. Such a support mechanism does not require a zero length spring. Due to this potential, the feasibility and advantages of using wrapping cams in an arm support mechanism was investigated.

1.5.2 General Cam Synthesis

Cam synthesis is the process in which the mathematical function that defines the desired behavior of the cam is used to calculate the required geometry of the cam. The wrapping cam synthesis procedure used for the following work was developed in [21, 22], but it is briefly presented here for the reader's convenience. The reader is referred to these works for a detailed derivation and discussion of the following procedure. Figure 7 depicts a common wrapping cam configuration in which the rope attached to the cam passes over an idler pulley. The rope on

this cam does not cross the line between the cam's center and the pulley's center, but such a "crossed configuration" is also common. While typically it is the cam that rotates, it is convenient to fix the coordinate system to the cam, so the pulley is depicted as rotating around the cam.

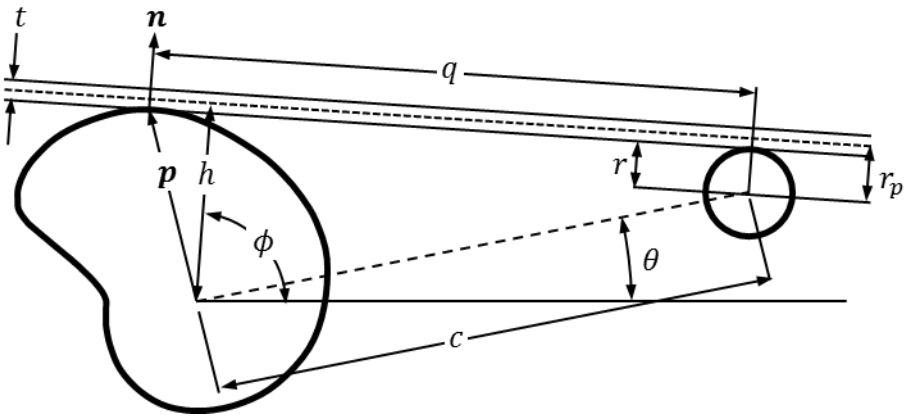

Figure 7. A typical wrapping cam in uncrossed configuration with dimensions and variables relevant to cam synthesis [21].

In Figure 7, $\boldsymbol{p}$ is the vector from the cam's center to its surface; $\boldsymbol{n}$ is the unit normal vector to the cam surface at $\boldsymbol{p}$; h is the length perpendicular to the rope from the rope's centerline to the cam's and can be thought of as the moment arm of the rope about the cam's center; c is the center distance between the cam and the pulley; q is the straight length of cable between the cam and the pulley; t is the thickness of the rope; r_p is the pitch radius of the pulley; r is the radius to the surface of the pulley, constrained by:

$$r = r_p - \frac{t}{2}\ ; \tag{2}$$

θ is the cam rotation in radians; and ϕ is the angle in radians from the centerline to a line perpendicular to the rope.

To define the surface of a cam, a series of points, $\boldsymbol{p}$, are calculated. The vector $\boldsymbol{p}$ is defined using complex polar notation as

$$\boldsymbol{p} = ce^{i\theta} \pm \left(r_p \mp \frac{t}{2}\right) e^{i(\theta+\phi)} + qe^{i\left(\theta+\phi+\frac{\pi}{2}\right)}\ ; \tag{3}$$

where the top operator in the ± and similar operators corresponds to the uncrossed configuration, and the bottom operator corresponds to the crossed configuration in this and all subsequent equations.

The rope length, *q*, is

$$q = \frac{c\ sin(\phi)}{\left(1 + \frac{d\phi}{d\theta}\right)}, \tag{4}$$

where,

$$\frac{d\phi}{d\theta} = -\frac{1}{\sqrt{c^2 - \left(h \mp r_p\right)^2}}\left(\frac{dh}{d\theta}\right). \tag{5}$$

The angle ϕ is

$$\phi = \cos^{-1}\left(\frac{\left(h \mp r_p\right)}{c}\right). \tag{6}$$

The strategy to determine *h* and its derivative varies with the design constraints of the cam. Theses equations are for the case that a positive rotation unwraps the rope from the cam, but they may be adjusted for the case that a positive rotation wraps the rope onto the cam. This results in the same geometry, but is practically useful for maintaining a consistent coordinate systems.

In the case that a function is being used to define the rotation of the idler pulley with respect to the rotation of the cam or vise versa, the cam moment arm, *h*, is

$$h = r_p \frac{d\psi}{d\theta}, \tag{7}$$

where ψ is the rotation angle of the pulley in radians. Likewise the derivative of the cam moment arm with respect to cam rotation is:

$$\frac{dh}{d\theta} = r_p \frac{d^2\psi}{d\theta^2}. \tag{8}$$

In the case that a function is being used to define an output force or torque, the cam moment arm, h, is calculated using a force balance:

$$h = r_p \frac{T_c}{T_p}, \tag{9}$$

where T_c is the torque on the cam and T_p is the torque on the pulley. The derivative of the cam moment arm with respect to cam rotation is then

$$\frac{dh}{d\theta} = r_p \frac{T_p \frac{dT_c}{d\theta} - T_c \frac{dT_p}{d\theta}}{T_p^2}. \tag{10}$$

1.6 Overview

This thesis presents research conducted in the interest of improving the wearability of arm support devices through reduction in their size, weight, and visibility. A novel support mechanism was sought, and wrapping cams were determined to be a possible alternative to traditional support mechanisms. Two different wrapping cam based mechanisms were investigated and tested as prototype arm supports.

The first mechanism, called the "series wrapping cam", uses a wrapping cam to drive the rotation of a second wrapping cam responsible for stretching a spring. This particular arrangement maintains a small mechanism and spring size. A two-DOF, wall-mounted arm support was constructed using the series wrapping cam. The prototype supports the arm in shoulder elevation, and passively allows elbow flexion. The development, design, prototyping, and testing of this prototype are discussed in detail in Chapter 2.

The second mechanism uses two cams near the elbow to increase or decrease the support provided to the shoulder joint based upon the degree of elbow flexion. This is accomplished through an application of the "simultaneous displacement" concept developed by [23]. A three-DOF, wall mounted arm support was constructed using this mechanism. The prototype supports the arm in shoulder elevation and elbow flexion and additionally features a passive vertical joint at the shoulder. The development, design, prototyping, and testing of this prototype are discussed in detail in Chapter 3.

2 Series Cam Mechanism Design and Testing

2.1 Series Cam Mechanism Overview

As discussed in the previous chapter, the goal of this research was to investigate the advantages and disadvantages of applying wrapping cams in an arm support mechanism. An initial mechanism concept utilizing wrapping cams was developed. Through a series of revisions, the series wrapping cam mechanism concept was developed. This mechanism features two wrapping cams which are connected to each other such that one drives the rotation of the other. This arrangement is advantageous because it gives the designer the freedom to simultaneously minimize both the size of the cam and the spring. A wall-mounted, prototype arm support was constructed utilizing the series wrapping cam mechanism to support shoulder elevation. An unsupported DOF at the elbow was included, making this an imperfect support device because it does not respond to elbow flexion. The torque profile of the series wrapping cam device was measured using a load cell and a potentiometer. The device exhibited the proper support torque profile for an arm balancer with some error due to friction, assembly error, spring characterization error, and rope elasticity.

2.2 Series Wrapping Cam Concept Development

In the interest of investigating the application of wrapping cams in arm support mechanisms, an initially simple wrapping cam mechanism was considered. This concept was revised multiple times until the series wrapping cam concept was developed. This series of concepts is described here to demonstrate the advantage of the series cam mechanism over simpler mechanisms.

2.2.1 Initial Fixed Cam Concept

The first concept considered, shown in Figure 8, was to fix a cam next to the user's shoulder. In this concept, a link placed parallel to the arm pivots about a horizontal axis through both the cam and the user's glenohumeral (GH) joint. A rope connects the cam and a spring attached to the supported link, so, as the supported link and upper arm are lowered, the rope wraps around the fixed cam at the shoulder and stretch the spring.

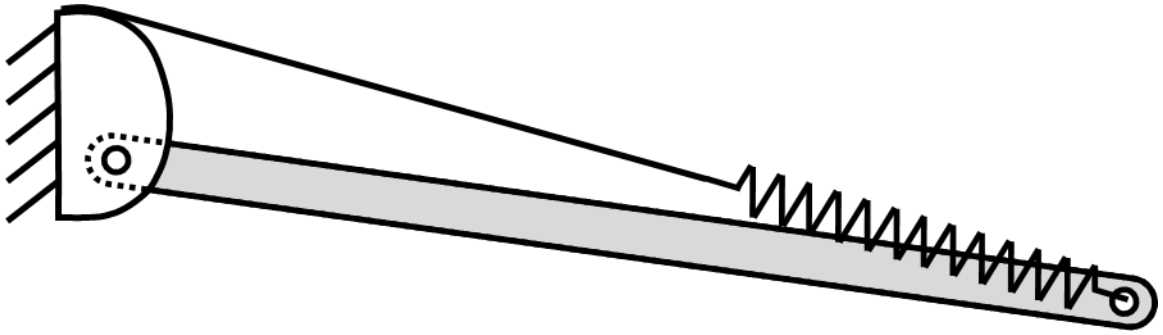

Figure 8. A simple arm support utilizing a single wrapping cam.

This was concept was disregarded for two reasons. First, the cam would need to have an excessively large radius or an excessively strong spring to create the large torque necessary to support a horizontal arm. Second, the moment arm of the cam would need to approach zero as the arm was lowered, and a cam could not be synthesized to meet these requirements given the limited cam rotation available to accomplish this.

2.2.2 Geared, Helical Cam Prototype

This concept was revised by adding a pair of gears to the mechanism, as shown in Figure 9. In this concept, a gear is fixed next to the shoulder with a mating pinion placed on the upper arm link. This pinion drives the rotation of the wrapping cam responsible for stretching the spring.

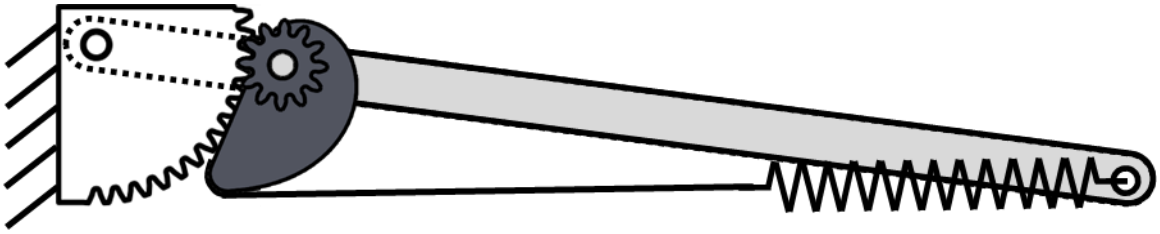

Figure 9. A gear-driven wrapping cam mechanism for arm support.

A simple prototype, shown in Figure 10, was created using 3D printed parts to demonstrate this mechanism. The gear ratio used was 4:1, so for a 90° rotation of the upper arm link, the cam rotates 360°. This ratio was selected to maximize the rotation of the cam, keeping the cam radius and spring size small. However, this full rotation causes the cam to rotate into its own rope. A helix was added to the perimeter of the cam, allowing the cable to pass next to the cam near the end of its rotation. Rubber bands were used for a spring element.

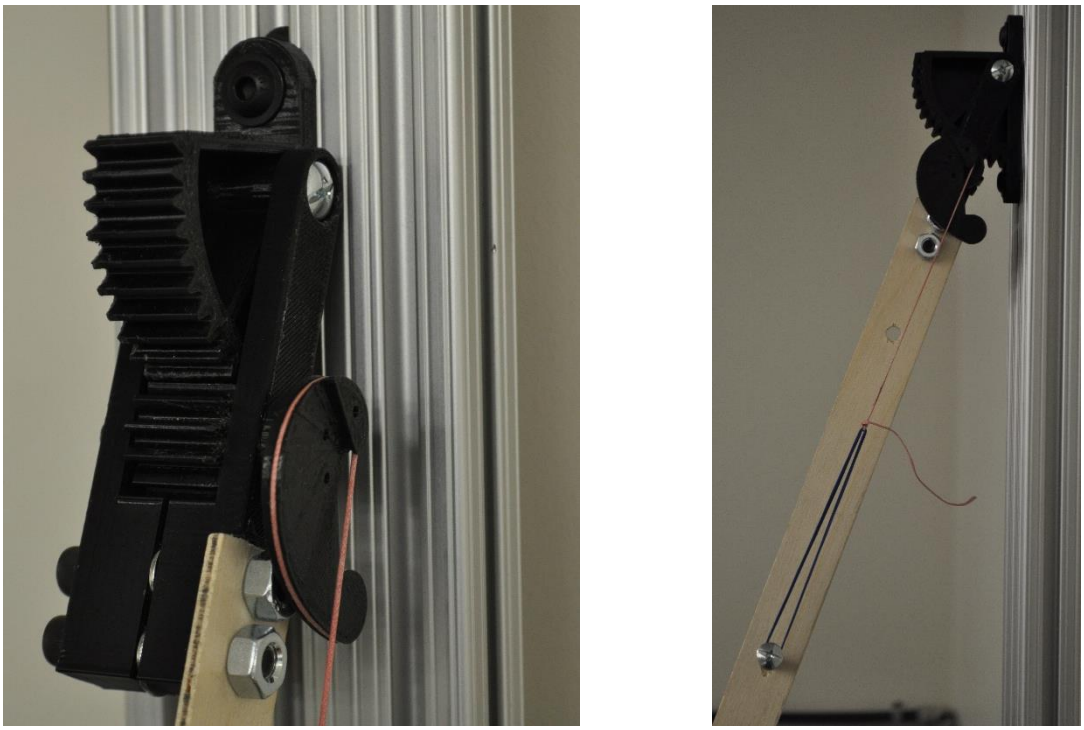

(a) (b)

Figure 10. Pictures of the gear driven wrapping cam gravity balance mechanism. (a) Close up of the gears and cam mechanism. The red rope is visible wrapping around the perimeter of the cam and passing by the side of the cam. (b) Side view showing the rest of the supported link and the attachment of the rubber band.

This prototype was qualitatively tested by mounting it to the wall and moving it through its range of motion by hand. The prototype successfully demonstrates the correct, sinusoidal torque profile for a balancer, but the 3D printed gears are not smooth. Thus, when the device is placed in its lowest position, where the support torque is lowest, there is too much friction for the support torque to overcome, and the link does not rise on its own. This friction and rough motion could be reduced with better gears and other components, but it was determined that using gears was not ideal for this application and that the helical cam is too impractical for manufacturing. Thus alternatives to the gears and the helical cam were sought.

2.2.3 Series Wrapping Cam Concept

Since a wrapping cam was already included in the design, it would be natural to replace the gear train with another wrapping mechanism. In its simplest form, the two gears could be replaced by two pulleys, a large one fixed next to the shoulder, and a smaller one attached to the supported link and fixed to a cam. A rope would terminate on both pulleys, so as the supported link is lowered, the rope would wrap around the pulley at the shoulder and unwrap from and turn the smaller pulley. This smaller pulley would then drive the rotation of the cam.

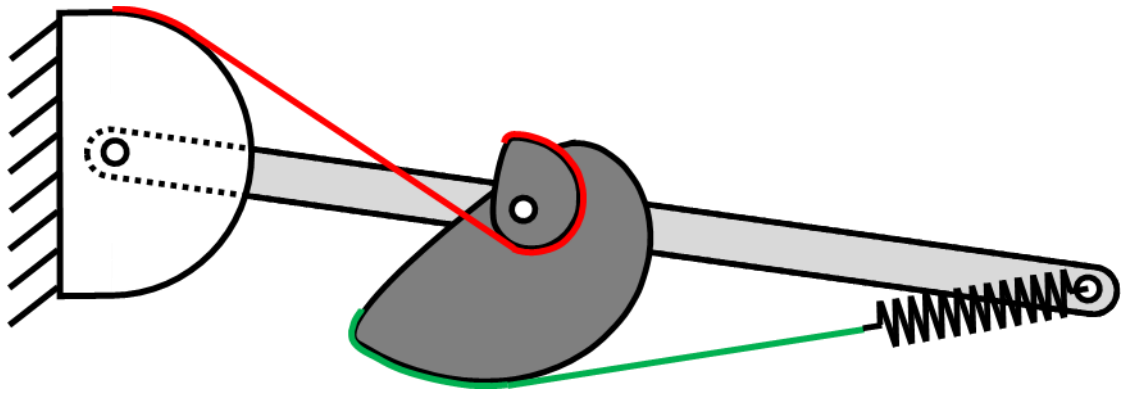

Figure 11. A diagram of the series wrapping cam mechanism. The drive rope, which wraps on the drive cam is shown in red. The spring rope, which wraps on the spring cam and attaches to the spring is shown in green.

However, using a cam in place of the smaller pulley, as depicted in Figure 11, is advantageous. This cam will be referred to as the drive cam, because it drives the rotation of

the other cam. The second cam will be referred to as the spring cam, because it causes the necessary deflection of the spring to store the arm's potential energy. This mechanism is called the series wrapping cam mechanism because the kinematic output of one cam is the input of the other. In this sense, a parallel wrapping cam mechanism would be one in which two or more cams shared an input but each had distinct outputs.

The drive cam can be designed with a small radius at the start of its rotation (when the arm is horizontal); at this point the arm needs its highest support torque, but the tension in the spring is at its lowest. The small radius gives the spring cam a high mechanical advantage, allowing a smaller spring cam and a lower initial spring tension. As the drive cam rotates, its radius can then increase. This decreases the mechanical advantage of the spring cam as the required support torque decreases. It also causes the spring cam to rotate less as the arm's change in potential energy is lower and less spring deflection is required. This eliminates the need for a helical cam by more effectively using a smaller cam rotation.

2.3 Series Wrapping Cam Synthesis

The series wrapping cams were synthesized in MATLAB (The Mathworks, Inc., Natick, MA) using the general procedure outlined in section 1.5.2. For each cam, 500 points were generated and saved for importing into SolidWorks as curves. The cam synthesis was carefully set up such that the two cam curves were correctly oriented to each other in the same coordinate system. The drive cam was synthesized using equations for unwrapping and the spring cam was synthesized using equations for wrapping. The MATLAB code for the cam synthesis is included in the Appendix.

2.3.1 Drive Cam Synthesis

As discussed in the previous section, the drive cam was designed to rotate the spring cam at an initially high but decreasing rate relative to the rotation of the upper arm. This behavior was defined using the following exponential position function:

$$\theta = c_3\left((\psi + c_1)^{\frac{1}{c_2}} - c_1^{\frac{1}{c_2}}\right), \tag{11}$$

where θ is the rotation of the cams; ψ is the downward rotation of the upper arm from the horizontal (also the rotation of the fixed pulley at the shoulder relative to the upper arm); and c_1 and c_2 are arbitrary constants. The exponent $1/c_2$ causes the rate of rotation to decrease as the arm is lowered as long as the constant c_2 is greater than 1. The constant c_1 was introduced into the function to allow adjustment of the initial slope of the curve which impacted the initial radius of the cam. The constant c_3 defines the maximum rotation of the cam and is defined as:

$$c_3 = \frac{\theta_{max}}{(\psi_{max}+c_1)^{\frac{1}{c_2}} - c_1^{\frac{1}{c_2}}}, \tag{12}$$

where θ_{max} is the maximum allowed rotation of the cam, and ψ_{max} is the maximum downward rotation of the upper arm from the horizontal.

The constants c_1, c_2, ψ_{max}, and θ_{max} were chosen experimentally in order to make the drive cam's initial radius slightly larger than the selected support shaft ($\varnothing$*=0.25 in*), to minimize the size of the spring cam, and to ensure feasible cam profiles. The rotation of the arm, ψ, was limited from 0-79° below the horizontal. This limitation was necessary because, beyond this angle, the spring cam synthesis yielded infeasible geometry. The output of this function is shown in Figure 12.

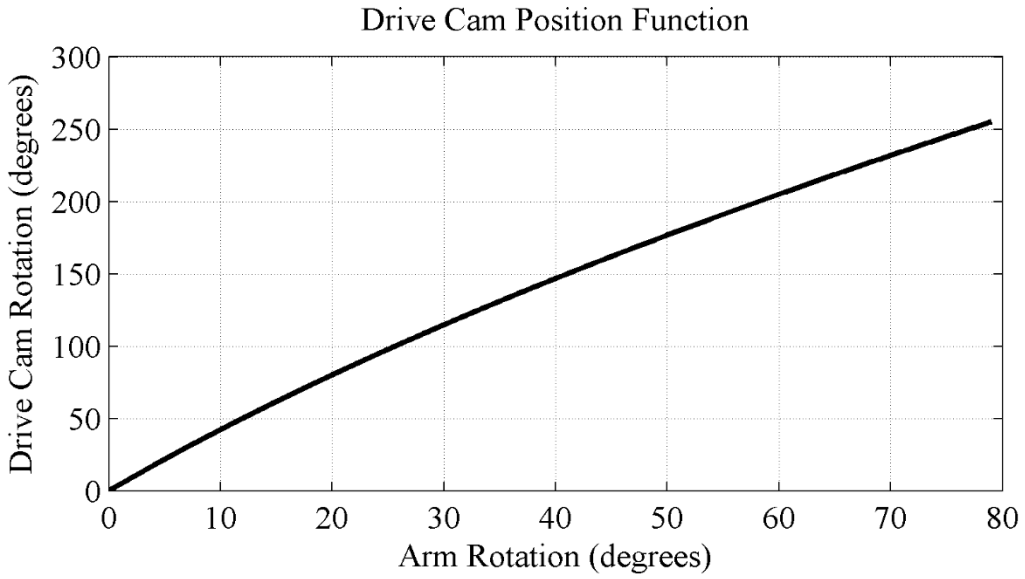

Figure 12. The position function used to define the output rotation of the drive cam plotted vs downward rotation of the upper arm from the horizontal.

2.3.2 Spring Cam Synthesis

The spring cam was synthesized using a procedure similar to the specified force function procedure outlined in Section 1.5.2. Two constraints were used to synthesize the spring cam. First, the spring cam must store the change in the arm's gravitational potential energy as elastic potential energy in the spring. Second, it must cause the appropriate torque at the shoulder joint to support the arm.

The first constraint was used to determine the position and consequently the tension of the spring. For the spring, a linear force-length relationship was assumed:

$$F = kx + F_0 \,, \tag{13}$$

where F is the spring tension; k is the spring rate; x is the length of the spring; and F_0 is force intercept at zero length. The energy balance with the arm horizontal as the initial state is

$$WLsin(\psi) = \frac{1}{2}k(x^2 - x_i^2) + F_0(x - x_i) \,, \tag{14}$$

where W is the weight of the arm, L is the distance from the center of the GH joint to the arm's center of gravity, ψ is the downward rotation of the arm from horizontal, and x_i is the initial length of the spring. Solving for x yields:

$$x = \frac{-F_0 + \sqrt{F_0^2 + 2k\left(WLsin(\psi) + \frac{1}{2}kx_i^2 + F_0x_i\right)}}{k}. \quad (15)$$

The second constraint was used to determine the torque on the series cam mechanism through a static force balance on the drive rope:

$$T = \left(\frac{WLcos(\psi)}{r_p}\right)h_d\,, \quad (16)$$

where T is the torque on the series cam, r_p is the radius of the fixed pulley, and h_d is the moment arm of the drive cam.

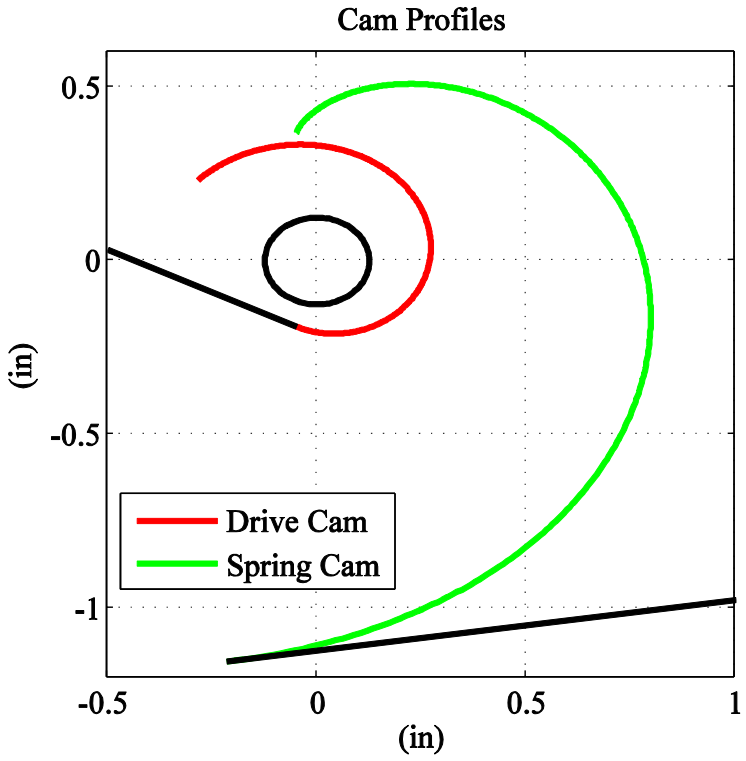

Figure 13. The series wrapping cam profiles. The shaft about which they rotate and their ropes are shown in black. This orientation corresponds to a horizontal arm when the drive cam is fully wrapped and the spring cam is fully unwrapped. As the arm is lowered, the cams rotate clockwise.

With both the torque on the drive cam and the tension in the spring known, the moment arm of the spring cam, h_s, can be found using a torque balance on the series cam:

$$h_s = \frac{T}{F}. \tag{17}$$

The resulting cam series wrapping cam profiles are shown in Figure 13.

2.4 Prototype Design and Manufacturing

2.4.1 Device Overview

A simple, prototype arm support, shown in Figure 14, was built to demonstrate the series wrapping cam as a gravity balance mechanism. For simplicity, the device is mounted to the wall and has only two DOF's. The pulley utilized by the series wrapping cam mechanism is fixed to a length of t-slotted framing mounted vertically to the wall. This allows the horizontal axis of the joint through the fixed pulley to be placed at the same height as the user's GH joint. The user must stand next to the shoulder joint to complete alignment with the device. A link, placed parallel to the upper arm, rotates with the upper arm about the center of the fixed pulley. This link is supported by the series wrapping cam mechanism.

Figure 14. The prototype arm support featuring the series cam mechanism shown supporting a user's arm.

A 3D printed bracket was fixed at the end of the supported link. This bracket wraps from the side of the arm to the underside of the elbow to a passive revolute joint. This joint allows the elbow to rotate about an axis perpendicular to the centerline of the upper arm and perpendicular to the axis of the revolute joint next to the shoulder. A final link, also 3D printed, extended beyond this joint underneath the forearm. Thermoplastic cuffs were attached to the two 3D printed parts to support the upper arm and forearm. The 3D printed module can be removed to facilitate measurement of the support torque without attachment to the arm. A detailed CAD model of the prototype is included in the supplementary files.

2.4.2 Cam Manufacturing

To manufacture the series cam mechanism, the coordinates generated by the cam synthesis were imported into SolidWorks as two curves for modeling and CNC machining of the cams. Because the series cams must be fixed to each other, they were machined out of a single piece of aluminum. The stock was held in alignment with a tooling plate by two dowel pins in through holes, allowing orientation to be controlled when flipping the part. The profile of the larger spring cam was machined first. Then the part was flipped, and the drive cam was machined. Grooves for the rope were machined with the cam flat on the tooling plate using a t-slot cutter. Cutouts were milled into the side of the cam to hold the rope terminals. These cutouts featured a pathway for the rope that ended tangent to the cam surface, ensuring that the rope wrapped over no sharp corners. The series cam is shown in Figure 15.

Because the pulley at the shoulder is only needed for a quarter turn, it was machined as a semicircle with a flat plate on one side for mounting to the t-slotted framing. As with the cams, a groove was cut to guide the rope using a t-slot cutter. A threaded hole was also machined into the bottom edge in alignment with the rope groove so that the drive rope could

terminate on an adjustment screw. A cutout was also machined into the side of the pulley to the end of the threaded hole so that a smooth, curved face exists to direct the rope into the center of the adjustment screw. The pulley is shown in Figure 16.

Figure 15. The series cam after machining.

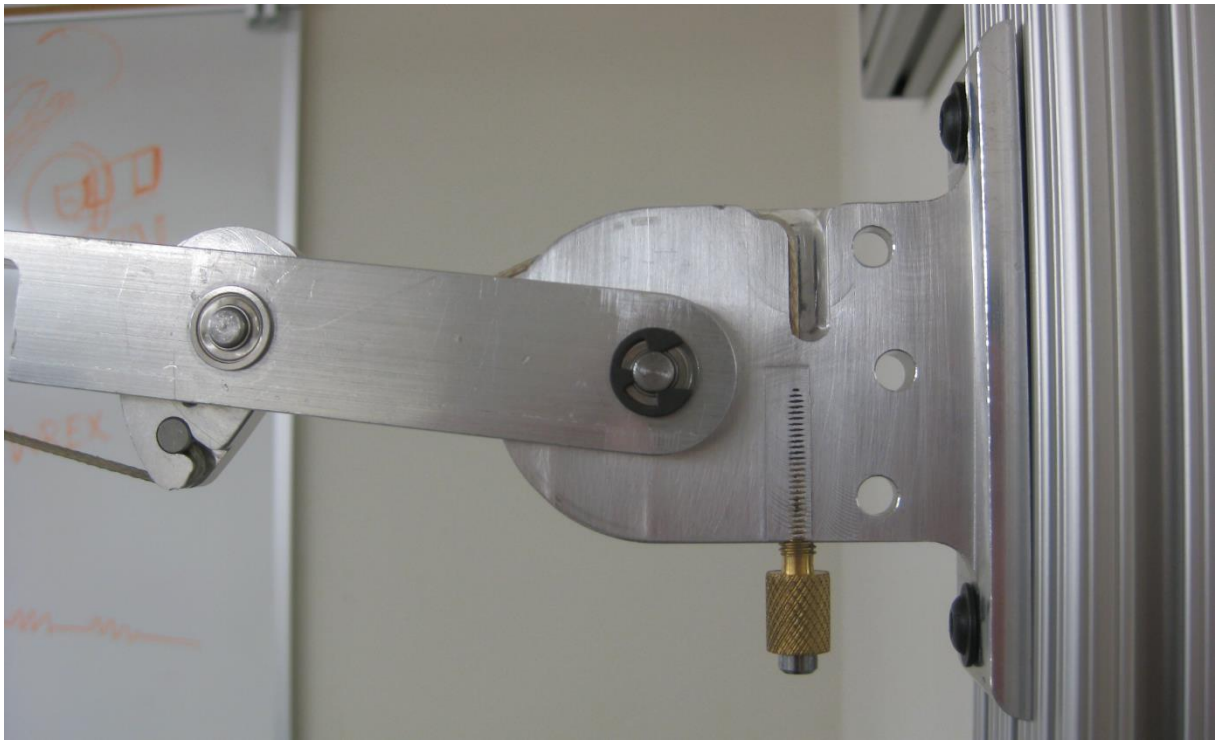

Figure 16. A close up of the series wrapping cam mechanism. The fixed pulley is shown on the right, with the supported link extending to the left. The spring cam is visible, but the drive cam is hidden inside the supported link.

2.4.3 Synthetic Fiber Rope Selection and Termination

Because steel wire rope is susceptible to bending fatigue when wrapped around a diameter less than 40 times its own diameter [24], it would not be suitable for wrapping around the very small radius of the drive cam. Synthetic fiber ropes were considered as an alternative to steel wire ropes. The material Vectran was ultimately selected due to its high modulus and low creep compared to other synthetic fibers and its superior bend tolerance compared to steel [25]. A 1/16 inch diameter, single braid, Vectran rope called Vectrus (Yale Cordage, Saco, ME) was used for all wrapping elements in the two prototypes. This rope has an average spliced break strength of 800 lbs, and a maximum work load of 160 lbs (factor of safety of 5) [26].

While this rope is remarkably strong, it can be significantly weakened by a poor termination. The strength listed above is based on the use of eye splices for terminations in which a length of rope is threaded back into its own core leaving a loop at the end of the rope [27]. This is one of the most efficient termination methods, but it leaves a significant length of rope unusable for wrapping applications. Thus, an efficient yet compact rope termination was sought.

Resin potted terminals were found to be the appropriate solution [27]. For this prototype, a short length of round steel bar stock was drilled through with a 1/16 inch diameter, 5° tapered end mill until the tapered hole was large enough to thread the rope through. This hole was drilled radially for terminals that would be placed in the cams and axially for terminals that would be placed in the adjustment screws. The terminal was then threaded onto the end of the rope. Tape was wrapped around the rope leaving a section of rope the length of the terminal exposed at the end. This section of rope was completely un-braided and splayed. Finally, the fibers in this section of rope were thoroughly coated with Devcon 2 Ton Epoxy (ITW Devcon,

Adhesives Danvers, MA), the tape was removed, and the epoxied end was pulled into the terminal until flush. Excess epoxy was then wiped off the terminal. Once cured, this process results in a strong, cone-shaped, composite structure within the steel terminal. Because the rope had to be threaded through the adjustment screws, some assembly of the prototype was required before the second terminal was potted on each rope. The rope terminals are shown in Figure 17.

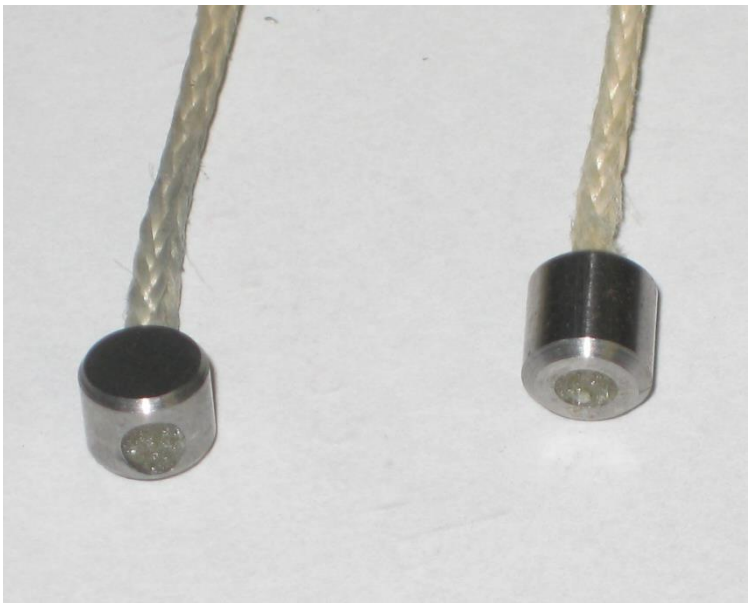

Figure 17. The two type of resin potted rope terminals. The terminal on the left is drilled through radially and is for terminations within cams. The terminal on the right is drilled through axially and is for terminations within adjustment screws.

2.4.4 Latex Spring Design

Steel coil springs would not be suitable for this application for a number of reasons. Particularly, they would be too large for a wearable device. In order for a spring to store a large amount of energy it must either have a very high spring rate or be able to stretch a large distance. Spring with high spring rates usually have unacceptably large diameters, and springs must be several times longer than their maximum deflection. In addition to being too large, steel springs would tend to be too heavy for a wearable application. Elastic bands were used as spring elements in the WREX [18], and a similar solution was sought for this prototype.

Latex was found to be a suitable alternative to steel coil springs. Latex has the capability to elastically stretch several times its own length without a helical coil like steel springs This allows the initial length of the spring to be quite small. Likewise, since it doesn't need to be coiled like steel springs, a latex spring can be thinner. Other materials, such as some polyurethanes, may have higher energy storage densities, but latex was selected because it is readily available in tube form.

According to the data provided by Primeline Industries (Akron, OH) [28], latex tubing exhibits a linear force/deflection relationship between 100% and 400% elongation. Because of this, the series wrapping cam was designed to utilize only this linear range in the tubing's range of motion. By experimentally adjusting the tubing parameters, an arrangement of six, one inch long segments of ⅛ inch ID, ¼ inch OD, latex tubing was selected for the spring. The use of six tubes allows the spring to generate sufficient tension to keep the radius of the spring cam small without using a very large cross section tube. This arrangement also keeps the final stretched length of the spring manageable. Additionally, it provides the potential to decrease the amount of support to ⅔ or ⅓ of the full support by removing two or four of the latex tubes respectively.

This volume of tubing is just enough to store the gravitational potential energy of the arm if stretched from 100% elongation to 400% elongation. This demonstrates a major advantage of the series wrapping cam. The traditional balancer requires the spring to be significantly pre-stretched, whereas the series cam mechanism adapts to the properties of the spring. This allows it to use the spring to its full potential and minimize the size of the spring.

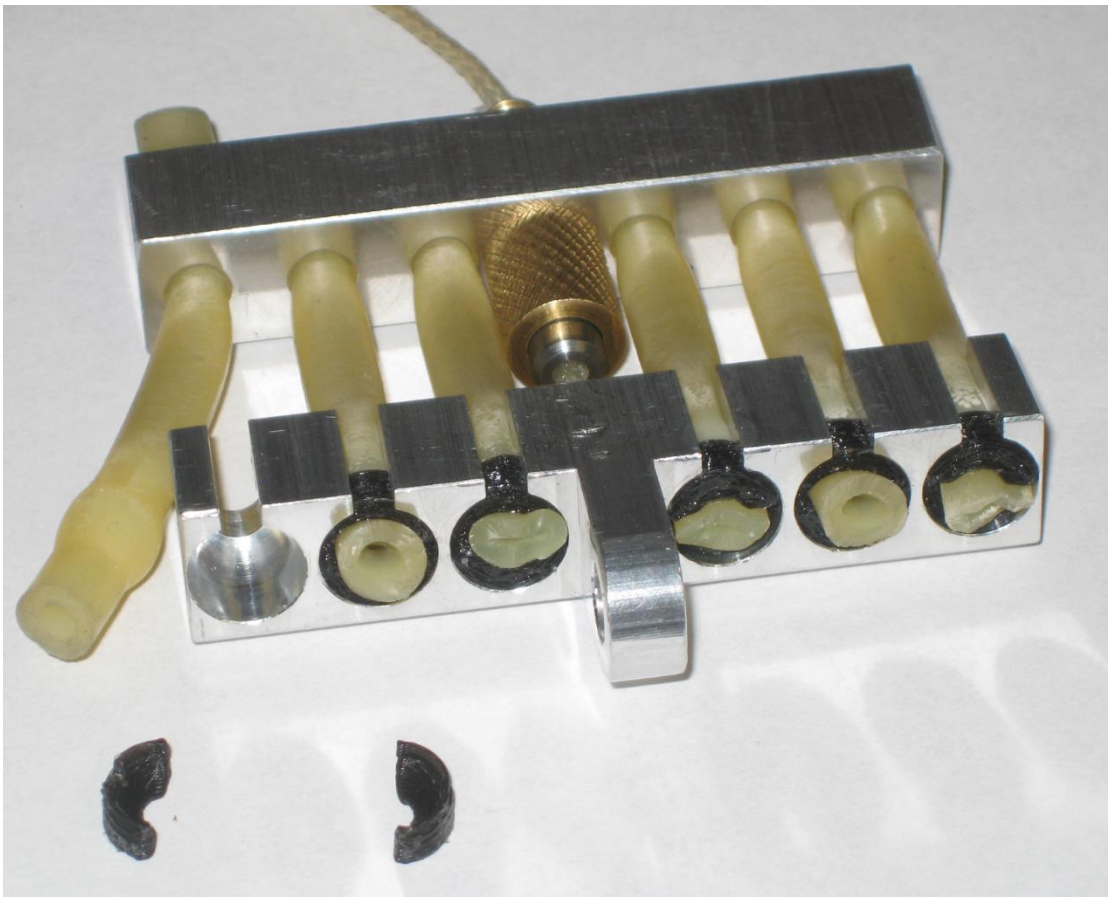

Figure 18. The custom spring built from latex tubing. The tube on the left is shown removed form the end plate to show the hemispherical cup in the endplate. A slight bulge in this tube is visible where the nylon ball sits. Two of the 3D printed wedges are visible on the bottom left.

The following method was developed to hold the six latex tubes together as a single spring. Nylon balls 3/16 inch in diameter were placed inside both ends of the tubes with the desired spring length of tubing between the two nylon balls. Additional tubing was left extending beyond the balls at each end. Two aluminum brackets were machined to hold each end of the tubing. Thru holes were drilled to allow the tubing to pass through, and a ball-nose end mill was plunged into the bracket to create a hemispherical cup concentric with the thru holes. Then a slot was cut from the sides into the cups and holes so that the tubing could be slipped into the cups from the side. Finally, the ends of the tubing with the nylon balls were pulled into the cups. In order to prevent the latex from pulling off of the balls, two small,

circular, 3D printed wedges were pressed into the cup, clamping onto the latex tubing above the nylon ball. One bracket was designed to mount on the frame of the device. The other bracket featured a threaded hole for the adjustment screw of the rope to the spring cam. The spring is shown in Figure 18.

2.4.5 Cam Adjustment

Because it would be too difficult to make the cam ropes exactly the necessary length, a mechanism to adjust the location of the cable terminations was necessary. This was achieved by threading one end of each cable through a bolt with an axial through hole. These hollow bolts also have a cup bored into their head to hold the steel cable termination. No slot was machined into the side of the bolt or the female threaded parts, so the rope had to be threaded through both of these parts before potting the second terminal. The rope was intentionally cut slightly long, to allow for adjustment.

The ropes for each cam must be independently adjusted after the device is fully assembled. To accomplish this, the upper arm link is held horizontal. Initially, the screw for the drive cam was adjusted until a line machined onto the series cam surface was perpendicular to the upper arm link. However, while testing the device, it was discovered that it was not capable of moving through its full 79° of rotation. Before it reached this angle, the spring cam would rotate beyond its intended range of motion, contact the spring rope, and stop the supported link. This is believed to be due to cable elasticity. The drive cable was adjusted in the position where the tension in the drive cable was at its maximum. This high tension caused the cable to stretch, and this elongation was removed in the adjustment. However, when the cable tension decreased as the device was lowered, the cable shortend, causing the series cam to over-rotate. To allow the mechanism to achieve its full range of motion, the drive rope length was increased until the

full range of motion was attainable. This gives the device its designed range of motion at the cost of reduced support accuracy in the early phases of its rotation. With the drive cam properly adjusted, the screw for the spring cam is adjusted until the initial stretch in the spring was at the designed value.

2.5 Device Testing

2.5.1 Qualitative Assessment

The device was qualitatively tested in two ways. First a weight was suspended from the end of the supported link. This provided a quick validation of the gravity support mechanism. Second, the prototype was used to support an arm. This allowed the user to experience the effect of the device as an arm support and evaluate its effectiveness and deficiencies.

The weight test demonstrated that the series cam mechanism works as a gravity balance mechanism. With the weight attached and adjusted to match the capability of the device, the supported link could be placed in any position, released, and then statically maintain nearly that position. Hysteresis was evident because the device would always move a few degrees in the opposite direction of its most recent motion before coming to rest.

Wearing the prototype also demonstrated the device correctly balanced an arm but had some shortcomings. When the elbow was fully extended, the device felt like it appropriately supported the arm at most elevations except horizontal, where it slightly under-supported the arm. Also, some hysteresis was noticeable in the device. When the arm was raised and then then allowed to rest on the arm support, the device would lower slightly before balancing the arm. The device felt smooth and would always rise from its lowest position without being pulled upward.

When the elbow was flexed, however, the device over-supported the arm. This was expected, as it was not designed to respond to elbow flexion. Trying out the device with this limitation, however, demonstrated that this was not an acceptable simplification for an arm support device. The work presented in Chapter 3 was conducted in order to eliminate this limitation.

2.5.2 Quantitative Torque Measurements

An experiment was conducted in order to quantitatively measure the torque generated by the device throughout its range of motion. The 3D printed, elbow module was removed from the supported link, and a single axis Phidgets 3134 load cell (Phidgets Inc., Calgary, AB), was attached to the end of the supported link with the direction of force measurement perpendicular to the link. A cable with a handle was attached to this load cell, so that a force could be applied to the load cell at a precise distance from the shoulder axis. A Bourns 6639S-1-103 potentiometer (Bourns, Inc., Riverside, CA) was connected to the shoulder axis to measure the position of the supported link. This test setup is shown in Figure 19.

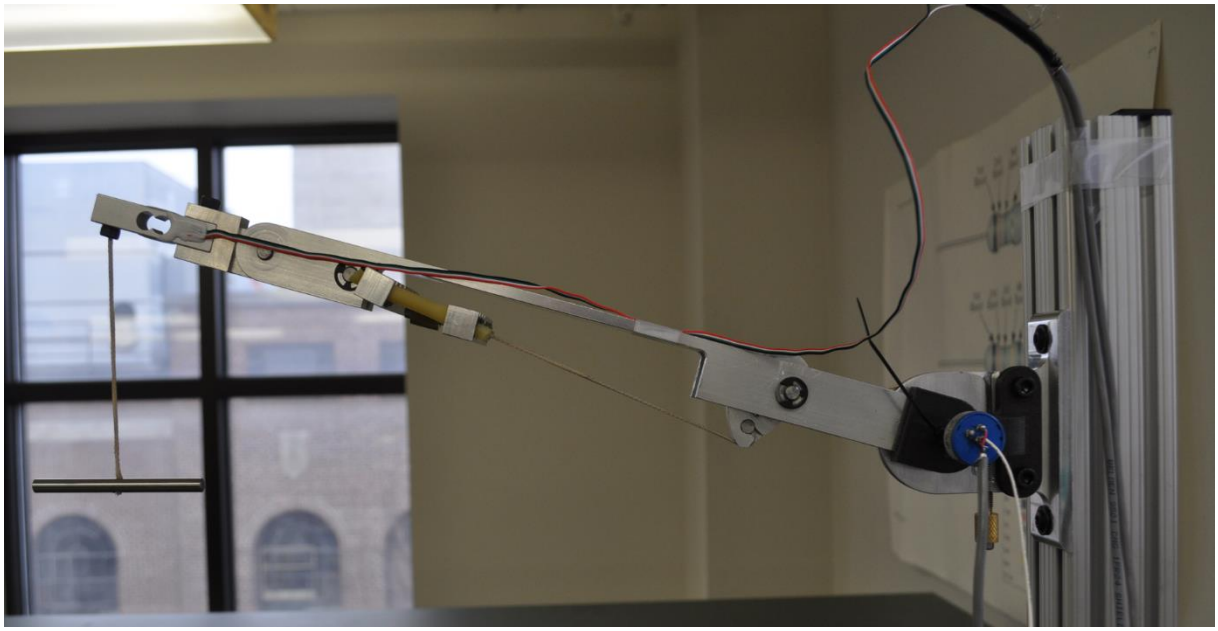

Figure 19. The experimental setup for measuring the torque profile of the series cam prototype.

Position and force were simultaneously recorded using MATLAB Simulink and an NI USB 6008 DAQ (National Instruments Corporation, Austin TX). First order low pass filters with a time constant of .05s (*fc=3.18 Hz)* were added to the Simulink program to reduce noise in the data. While recording, the device was pulled slowly from its rest position down to the lowest point in its range of motion using the cable attached to the load cell and then raised again to its rest position. The resulting torque profile is shown Figure 20.

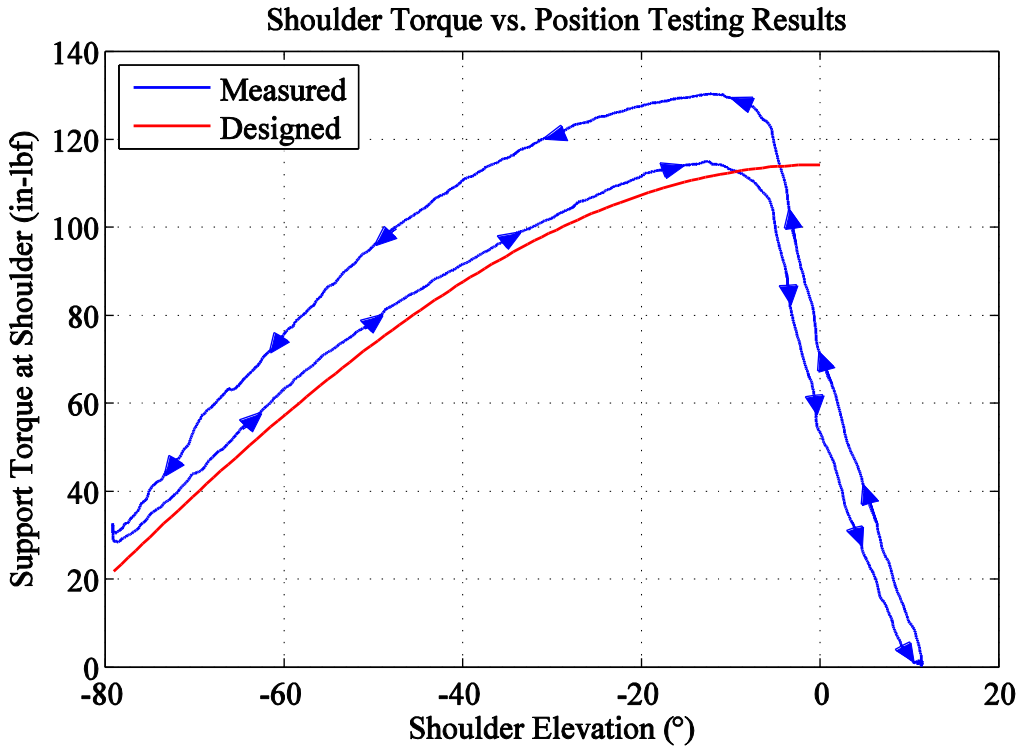

Figure 20. Testing results of the series wrapping cam mechanism. The arrows on the measured torque line indicate the direction of travel. A shoulder elevation of 0° corresponds to a horizontal upper arm and a shoulder elevation of -90° corresponds to a fully lowered upper arm.

Three errors in the device behavior should be noted. First, the support torque doesn't reach its maximum value when the supported link is horizontal as it is designed to. This due to the readjustment of the drive cable to allow full range of motion described in section 2.4.5. Second, the device consistently over supports. This could be caused by making the latex tubes in the spring too short, or the data from [28] may not accurately represent the actual behavior

of the tubing used. Third, significant hysteresis is present. The most dominant source of this hysteresis is likely friction in the terminals of the latex tubing. Other potential sources could be inelastic behavior in the latex, friction in the braided rope when wrapping, and friction in the bearings. A detailed analysis of each components contribution was not conducted.

2.6 Discussion

The series cam mechanism has the potential to reduce the size and weight of spring based orthoses. Cams allow the device to supply a custom torque profile. The use of two cams gives the designer the freedom to minimize both the size and initial tension of the spring as well as the size of the cam.

The prototype presented in this chapter successfully demonstrated the application of the series wrapping cam mechanism in an arm support device. The prototype exhibited the general torque vs. position behavior of a gravity balance mechanism. However, significant error was present. Some potential measures could be taken to reduce this error. Stretch of the drive cable could be incorporated into the synthesis. Error in the spring behavior could be reduced through more precise manufacturing and assembly as well as careful characterization of the resulting spring. A lower friction termination for the latex tubes could reduce the hysteresis in the device. The overall behavior of the spring may also be improved by casting a custom spring from urethane or a similar material rather than assembling latex tubes. This spring could be significantly smaller than the latex tubing both because it wouldn’t be composed of multiple, spaced-out tubes and because some urethanes have the ability to stretch even more than the latex tubing used in this prototype. Possibly, the ends of the spring could be cast from a rigid urethane to minimize friction in the termination, and the middle could be cast from a more

flexible urethane. Preventing the spring from tearing at the interface of two different types of urethane would be a challenge in this design.

The prototype is not particularly low profile. The largest reason for this was the horizontal orientation of the spring. However, the spring was placed in this orientation simply to make the prototype easy to machine. A frame could be made to accommodate a vertically oriented spring, which would allow the device to reside much closer to the arm.

The largest drawback of this prototype is that it does not respond to elbow flexion. Wearing the prototype clearly demonstrated that this simplification does not yield a satisfactory arm support as the user must apply a significant downward torque to the device when the elbow is flexed. Chapter 3 describes a new mechanism designed to accomplish this coupling between elbow flexion and the support provided to the shoulder. Ultimately, the series wrapping cam was not incorporated into this design. However, the series wrapping cam is a potentially useful mechanism for other spring based orthoses. For example, it could be applied to a cable based hand orthosis for stroke victims with hypertonia, which would also require a custom torque profile which is not achievable with normal springs [29].

3 Simultaneous Displacement Cam Mechanism Design and Testing

3.1 Simultaneous Displacement Cam Mechanism Overview

The qualitative testing of the series cam mechanism, discussed in 2.5.1, demonstrated clearly that an arm support that does not respond to elbow flexion is unsatisfactory. Therefore a method to couple elbow flexion with the support torque at the shoulder was sought. A method for energy free adjustment of traditional gravity balancers was adapted for this purpose. This method, called simultaneous displacement [23], requires that both endpoints of the support spring be moved such that the length of the spring remains constant. This simultaneous displacement of the spring's endpoints is actuated with two cams coupled to the flexion/extension of the elbow. A cam mechanism is used to simulate the zero length spring of the gravity balancer. This mechanism is mounted on linear guide rails so that they can freely translate as actuated by the cams at the elbow. A wall-mounted prototype arm support was built to demonstrate this concept. The prototype has a passive vertical DOF above the shoulder, a supported horizontal DOF at the shoulder, and a supported DOF at the elbow. The prototype was tested in multiple configurations using a potentiometer and a load cell. The coupling of the elbow to the upper arm support was successfully demonstrated. A very significant amount of friction is present in the elbow joint and its associated mechanisms.

3.2 Ideal Balancing of an Arm without a Parallelogram Linkage

As discussed in 1.2, gravity balancing of multiple links in series, such as a person's upper arm and forearm, is traditionally accomplished by using parallelogram linkages for all but the most distal link. This is the method used by the WREX [18]. A different method was sought for two reasons. First, a solid frame from the shoulder to the elbow could possibly be made smaller and be more easily enclosed. Second, the traditional method requires a link that

wraps underneath the elbow to a vertical joint and then a second link that wraps back to the side of the forearm for the second gravity balancer. If the link supporting the forearm could remain underneath the forearm, the device would be significantly less visible and less likely to collide with the user's environment.

In order to simplify the mechanism needed to achieve this coupling, a degree of freedom at the shoulder was sacrificed. The arm support would have a vertical revolute joint through the GH joint, a horizontal revolute joint through the GH joint, and a revolute joint at the elbow perpendicular to both the upper arm's centerline and the horizontal revolute joint. This would still allow 3-DOF placement of the user's hand (plus 3-DOF orientation of the hand through rotation of the wrist beyond the device), but the arm would no longer have an extra degree of freedom to allow multiple configurations. Thus, the user would no longer have freedom to place the elbow in different locations for a given hand placement. This limitation is not ideal, especially for interactions with obstacles such as a table. However, adding a fourth degree of freedom may be possible once a prototype of a simpler device is built and demonstrated.

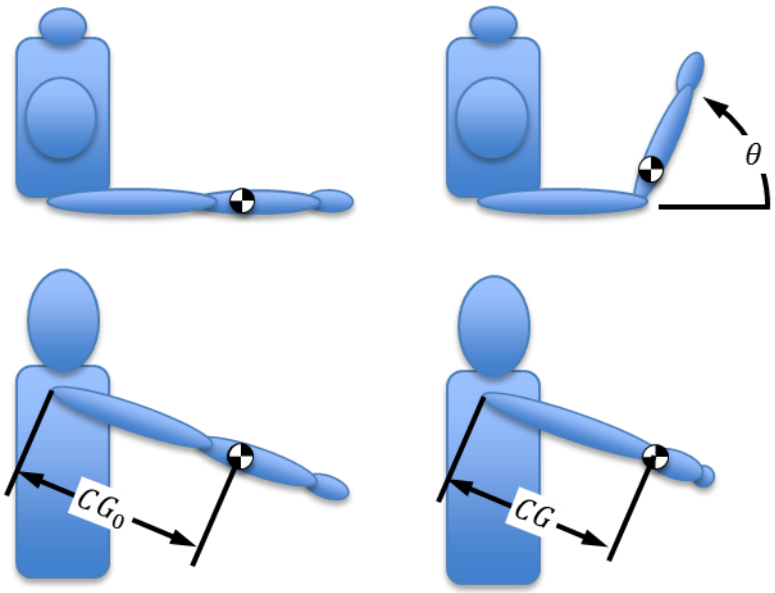

Figure 21. Movement of the arm's center of gravity as a result of elbow flexion. The shoulder is restrained to prevent shoulder rotation. Thus, when viewed from the side, the forearm is always aligned with the upper arm.

With this degree of freedom in the shoulder restrained, the projection of the entire arms center of gravity onto the vertical plane of the upper arm must remain on the centerline of the upper arm, as shown in Figure 21. Thus the torque about the shoulder for a given elbow flexion, T_{sh}, is

$$T_{sh} = CGcos(\theta_{sh}) , \tag{18}$$

where CG is the distance of the arm's center of gravity from the shoulder projected onto the vertical plane of the upper arm, and θ_{sh} is the angle of the upper arm from the horizontal. For any given elbow flexion, the distance of the arm's center of gravity from the shoulder will be some fraction of its maximum value at 0° elbow flexion. Thus, this fraction f_{CG}, is,

$$f_{CG} = \frac{CG}{CG_0}, \tag{19}$$

where CG_0 is the distance of the arm's center of gravity from the shoulder when the elbow is fully extended. Thus for a given elbow flexion, the torque at the shoulder is scaled from its maximum value:

$$T_{sh} = f_{cg} CG_0 \cos(\theta_{sh}) . \tag{20}$$

This behavior is illustrated in Figure 22. The exact relationship of the arms' center of gravity location to the degree of elbow flexion is discussed in more detail in Section 3.4.1.

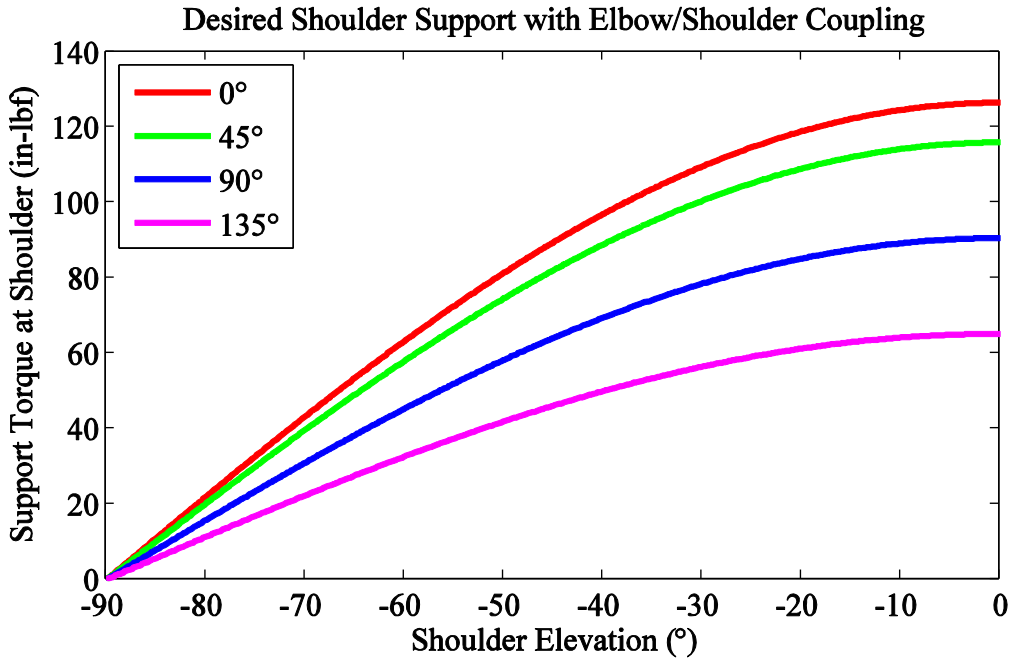

Figure 22. The desired behavior of the proposed arm support's shoulder support mechanism. The different colored lines represent different degrees of elbow flexion as noted in the legend, where 0° flexion corresponds to a straight arm. A Shoulder elevation of 0° corresponds to a horizontal arm and -90° corresponds to a completely lowered arm.

The kinematic constraint at the shoulder constrains the elbow to rotate in a plane inclined at the angle of the upper arm's center of gravity. When the upper arm is horizontal, the forearm could rest on this plane and no joint torque should be required to flex or extend the elbow. However, as the upper arm is lowered, a sinusoidal assistance in elbow flexion is required, which must be scaled to a maximum when the upper arm is vertical. Thus the torque at the elbow, T_{el}, is

$$T_{el} = \sin(-\theta_{sh})\left(CG_f \sin(\theta_{el})\right), \tag{21}$$

where CG_f, is the distance of the center of gravity of both the forearm and the hand from the elbow, and θ_{el} is the degree of elbow flexion from a fully extended arm. This behavior is shown in Figure 23.

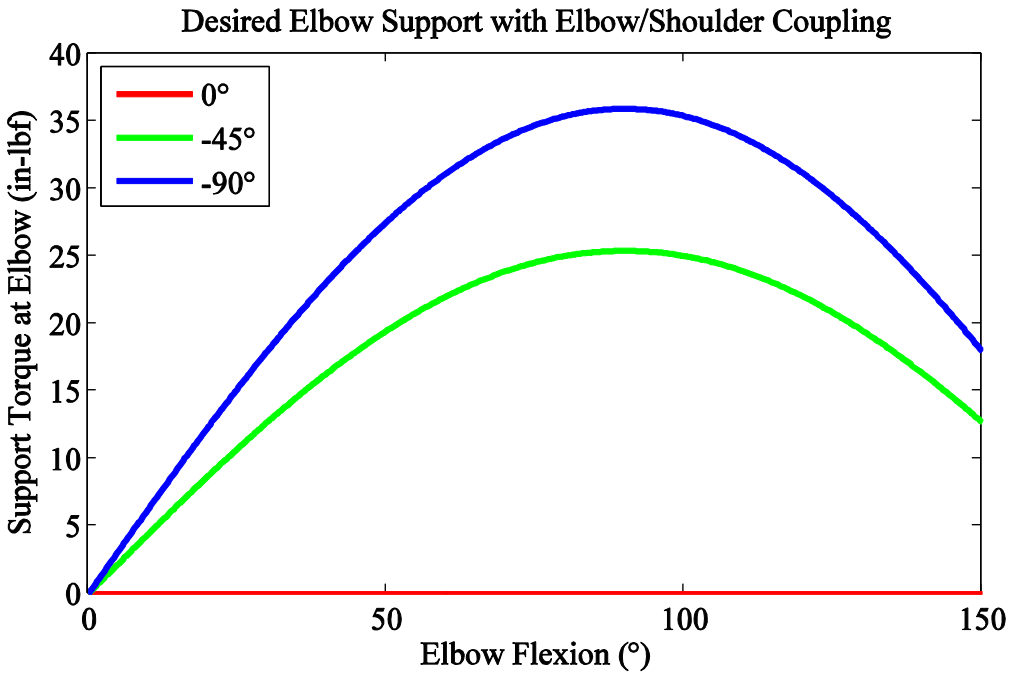

Figure 23. The desired behavoir of the proposed arm support's elbow support mechanism. The different colored lines represent different shoulder elevations as noted in the legend, where 0° corresponds to a horizontal arm, and -90° corresponds to a completely lowered arm. 0° elbow flexion corresponds to a straight arm.

3.3 Simultaneous Displacement Cam Concept Development

Various methods to achieve the desired shoulder/elbow coupling described in Section 3.2 were considered. Initially, modifications of the series wrapping cam mechanism were considered, chiefly the use of antagonistic quadratic wrapping cams [30]. No satisfactory modification of the series cam mechanism could be found. Instead, a traditional gravity balancer was modified using the simultaneous displacement method for energy free adjustment described in [23].

3.3.1 Application of Antagonistic, Quadratic Wrapping Cams in the Series Wrapping Cam Mechanism

This section briefly describes why the series cam mechanism was not used in the second prototype. The series cam mechanism specifies the stretch of the spring for a given arm position. Thus, the only way to accurately scale the support torque profile provided by the series cam

would be to scale the force/deflection relationship of the spring. Thus, if the spring had the following behavior when the arm was fully extended:

$$F = kx + F_0 \,, \tag{22}$$

then its behavior would need to be scaled in the following manner when the elbow was flexed:

$$f_{CG}F = f_{CG}(kx + F_0) = \alpha kx + \alpha F_0 \,. \tag{23}$$

Continuously adjusting the rate of a spring is a non-trivial design challenge.

One potential solution is to use the antagonistic quadratic wrapping cam mechanism described in [30]. This mechanism has two wrapping cams, each connected to a spring, that each generate a torque with a quadratic relationship to rotation. These cams are placed in opposition to each other such that the combination of the two torque profiles yields a linear torque profile. The cams can be rotated in opposite directions without turning the drive pulley, which was accomplished with a bevel gear in [30]. Adjusting this offset then adjusts the slope of the combined, linear torque profile.

It would be possible to replace the spring used in the series cam mechanism with quadratic, antagonistic wrapping cams. Cams actuated by elbow flexion could be used to change the offset of the quadratic cams. This would scale the simulated spring rate and consequently the torque generated by the series wrapping cam mechanism.

A MATLAB script was written to synthesize antagonistic, quadratic wrapping cams; however, no acceptably small combination of springs and cams was found. The quadratic function causes the cam radius to become unacceptably large for a wearable application near the cams' extreme rotation. Increasing the strength of the springs attached to each quadratic cam does decrease the size of the cam. However, in order to use a reasonably small cam, it was

found necessary to use an unacceptably large spring. Due to this difficulty, another method was pursued.

3.3.2 Review of Energy Free Adjustment Mechanisms

A number of methods exist to adjust a traditional gravity balancer without the input of energy. As discussed in 1.2, three parameters may be altered to adjust a standard gravity balancer: the distance between the spring attachment to the base link and the rotation axis, *a*, the distance between the spring attachment to the supported link and the rotation axis, *r*, and the spring constant, *k*. Spring-to-spring balancing, as it is referred to in [31], adjusts one of the support spring attachment locations. The attachment point is placed on a rail and attached to a second spring, which balances the force exerted along the rail by the support spring. The virtual spring concept method, as it is referred to in [32], adjusts the spring rate. This is accomplished by simulating the support spring with two springs placed at an angle to each other. The springs' attachments to the base link are repositioned in such a way that the springs' lengths do not change but the angle between them changes. The simultaneous displacement method, as it is referred to in [23], adjusts both spring attachment locations in such a manner that the length of the support spring remains constant. A simple way to accomplish this would be to temporarily place a rigid link between the two spring attachment locations, adjust their positions, lock them in their new positions, and then remove the rigid link.

Regardless of the method used, conservation of energy dictates that a gravity balancer can only be indefinitely adjusted without energy input if the supported link is returned to one specific orientation for this adjustment [23]. Imagine a support mechanism that could be indefinitely adjusted to varying loads in two positions. A weight could be placed on this mechanism in one position and lifted without any work to the second position. The weight could

then be removed and the mechanism adjusted to supply no support. The mechanism could be lowered to the first position without any energy input, and a second weight could be placed on it. With the mechanism adjusted to support the second weight, the process could be repeated, lifting an endless series of weights to the upper position without any energy input. This is clearly impossible.

3.3.3 Application of Simultaneous Displacement for Shoulder Torque/Elbow Flexion Coupling

The mechanisms for energy-free adjustment of gravity balancers described in Section 3.3.2 could be adapted to achieve the desired coupling of shoulder support with elbow flexion. As discussed in Section 3.2, when the arm is horizontal, the elbow should be able to move freely while shoulder support is adjusted. This adjustment, therefore, requires some energy free mechanism. Additionally, some mechanism would need to be in place to map from the degree of elbow flexion to the appropriate adjustment of the balancer. Wrapping cams are an appropriate mechanism to achieve this mapping because they can output an arbitrary function.

This coupling of elbow flexion with the energy free adjustment mechanism has an interesting consequence. If the elbow is given the freedom to flex/extend, adjusting the support mechanism for the shoulder, when the arm is not horizontal, it will require an energy input. Conservation of energy shows that this energy input is equal to the change in gravitational potential energy of the forearm as it is flexed/extended. Thus, the device would perfectly gravity balance the forearm. This can be shown by considering adjustment of the shoulder support only when the arm is horizontal. The elbow may be placed in any orientation without effort due to the energy free adjustment mechanism. Then, with the elbow held in that position, the arm may be lowered and raised with no effort due to the adjusted gravity balancer providing support to

the shoulder. This shows that any configuration of both the upper arm and the forearm can be reached with no effort from the user.

Ultimately, the simultaneous displacement method was selected for this mechanism. The virtual spring method was disregarded due to its complexity and bulk. Spring-to-spring balancing was considered to be the simplest option, but preliminary cam synthesis yielded infeasible cam profiles that could not be resolved. The simultaneous displacement mechanism, while complicated, has the advantage of using only the spring of the gravity balancer. Thus, the entire arm could be ideally balanced with one spring.

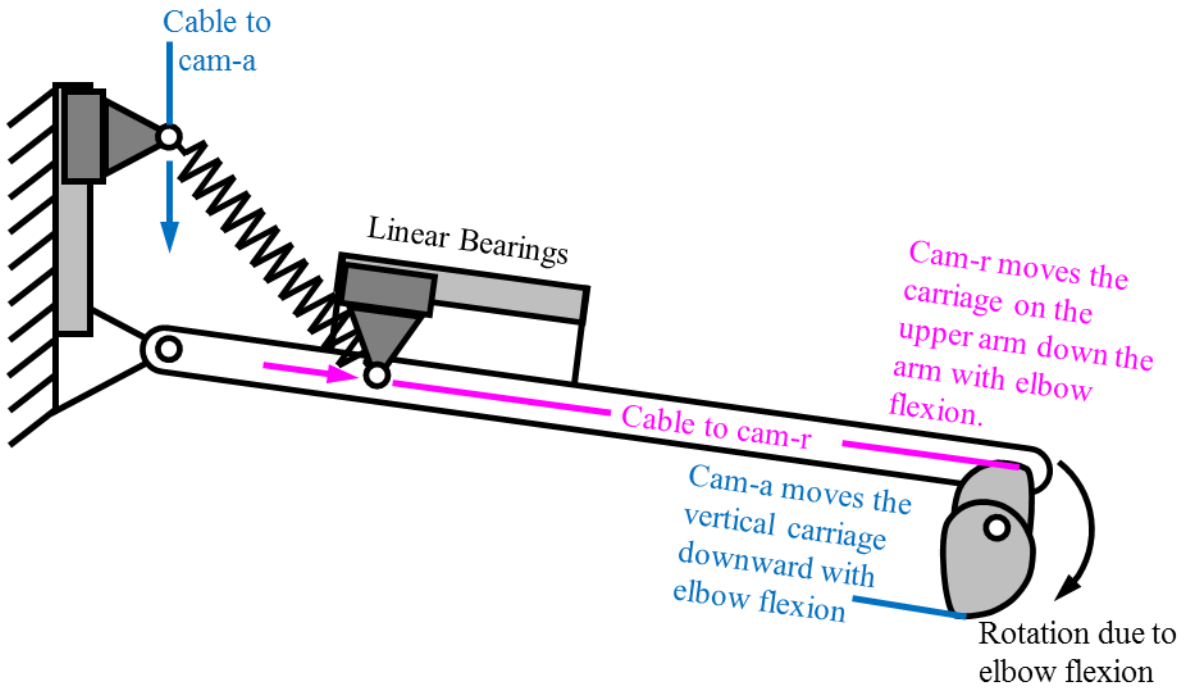

Figure 24. A diagram illustrating the simultaneous displacement cam mechanism. The cable that controls the attachement distance, *a*, is shown in blue, and the cable that controls the attachment distance, *r*, is shown in magenta. For simplicity, the cable routing from cam-a is to spring attachement-a as well as the link placed underneath the forearm are not shown. Details of the cable routing are discussed in more detail in Sections 3.5.3 and 3.5.4.

Obviously, if the simultaneous displacement mechanism were to be applied in a manner that allowed continuous adjustment while moving the supported link, a rigid link could not be placed on the support spring as described in Section 3.3.2 and [23]. Instead, two wrapping cams

are used to simultaneously control the position of both of the support spring attachment points, simulating the behavior of a rigid link when the arm is horizontal but allowing the support spring to stretch when the upper arm is lowered. One cam adjusts the distance from the rotation axis to the spring attachment to the base, *a*, and the other cam adjusts the distance from the rotation axis to the spring attachment to the supported link, *r*. Thus, these two cams are referred to as cam-a and cam-r respectively. These cams are also responsible for mapping the elbow flexion to the proper amount of adjustment to the shoulder support mechanism. This arrangement is shown in Figure 24.

In addition to the two cams for the simultaneous displacement mechanism, it was found to be beneficial to use a cam to simulate the support spring, as shown in Figure 25. To accomplish this, a carriage frame is attached to the linear guide rail to hold both the spring and the spring cam. A drive pulley is fixed to the spring cam, and a drive cable terminates on this pulley. This drive cable then passes over an idler pulley attached to the vertical, linear guide rail, then passes back down to a final pulley directly next to the drive pulley but fixed to the spring carriage. This pulley arrangement maintains a constant wrap angle so that the spring cam would only rotate relative to the carriage in response to a change in the distance between the drive pulley and the idler pulley. Thus the spring cam is able to simulate the zero length spring of a traditional balancer. Use of the spring cam provides a mechanical advantage that allows a smaller spring with less initial stretch to be used. For a more complete depiction of these mechanism, see the CAD models of the prototype included in the supplemental files. Rope are colored using the same conventions as those in Figure 24 and Figure 25.

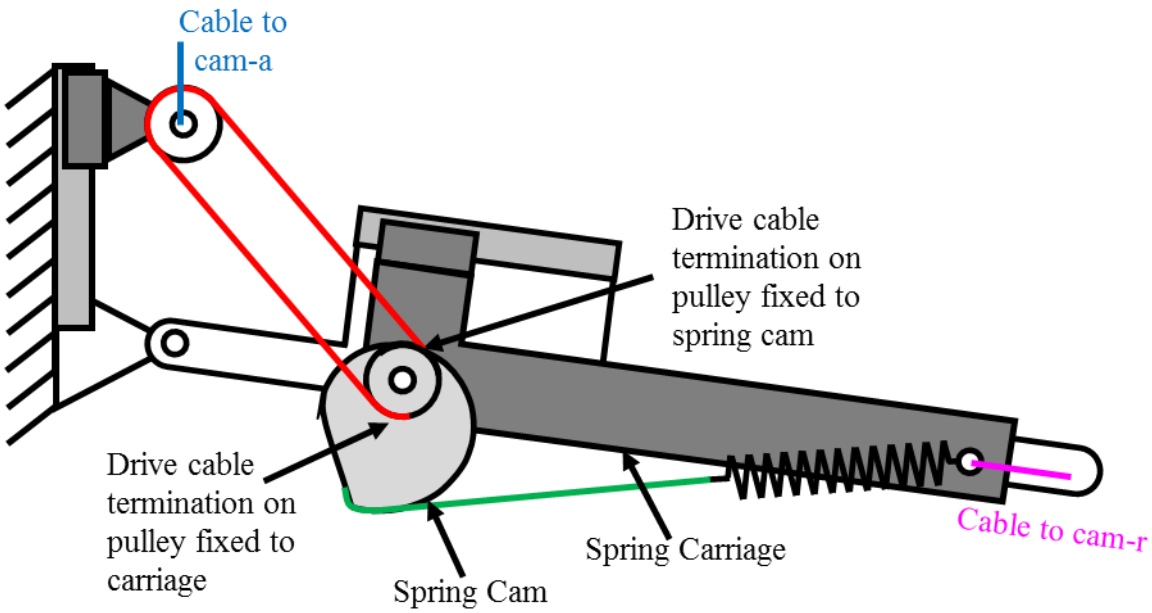

Figure 25. A diagram of the cam mechanism used to simulate a zero length spring. The drive rope is shown in red, and the spring cam rope is shown in green. The cables controlling the carriage locations are shown, but for simplicity, their routing the their cams are excluded.

3.4 Cam Synthesis

The cams for the simultaneous displacement mechanism were synthesized using a similar procedure as that used to synthesize the series wrapping cams. The MATLAB code for the cam synthesis is included in the Appendix.

3.4.1 Simultaneous Displacement Cam Synthesis

For the cam syntheses, the device home configuration was considered to be with the arm horizontal and the elbow fully extended. The simultaneous displacement cams were synthesized to adjust the two endpoints of the support spring as the elbow was flexed. With the elbow flexed, the support to the shoulder needs to only supply a fraction of the support that it does in the home configuration. This fraction of support was found using estimates of both the arm segment and mechanism link weights and centers of gravity (CG's). Segment weights and CG's, shown in Table 1, were estimated as averages of the data in [33-36]. Mass properties of the prototype links were calculated using the mass properties tool in SolidWorks.

Table 1. Anthropometry data used for the cam syntheses.

	Upper Arm	Forearm	Hand
Distance from proximal joint to center of gravity as percentage of segment length	47.5%	41.7%	47.0%
Segment weight as percentage of total body weight	2.86%	1.73%	0.691%

As discussed in Section 3.2, the projection of the forearm's center of mass onto the vertical plane of the upper arm is always on the center line of the upper arm. Thus the projected distance of the center of gravity of both the device and the arm from the shoulder, CG, can be found as

$$CG = \frac{W_u CG_u + W_f\left(L_u + CG_f \cos(\theta)\right)}{W_a}, \tag{24}$$

where W_u is the combined weight of the upper arm and its supporting link; CG_u is the distance from the shoulder to combined center of gravity of the upper arm and its supporting link; W_f is the combined weight of the forearm, hand, and their supporting link; L_u is the length of the upper arm; CG_f is the distance from the elbow to the combined center of gravity of the forearm, hand, and their supporting link; θ is the degree of elbow flexion from full extension; and W_a is the combined weight of the entire arm and both supporting links. The fraction of support for a given elbow flexion, f_{CG}, would be:

$$f_{CG} = CG/CG_0\,, \tag{25}$$

where CG_0 is the distance from the shoulder to the arm's center of gravity when the elbow is fully extended. The first and second derivatives of $f_{CG,}$ necessary for cam synthesis, are

$$\frac{df_{CG}}{d\theta} = -\frac{W_f CG_f \sin(\theta)}{W_a CG_0} \tag{26}$$

and

$$\frac{d^2 f_{CG}}{d\theta^2} = -\frac{W_f CG_f \cos(\theta)}{W_a CG_0}. \tag{27}$$

It is necessary to define the mathematical relationship between the support fraction, f_{CG}, and the adjustment to the support spring attachment locations, a and r. Two requirements must be satisfied. First, the amount of support provided must be scaled by f_{CG}. Thus,

$$ark = f_{CG} a_0 r_0 k \,, \tag{28}$$

or

$$a = \frac{f_{CG} a_0 r_0}{r} \,, \tag{29}$$

where a is the distance from the rotation axis to the spring attachment to the base link as a function of elbow flexion; r is the distance from the rotation axis to the spring attachment to the supported link as a function of elbow flexion; k is the spring constant; and a_0 and r_0 are the two attachment distances at full elbow extension. The second requirement is that the spring remain the same length throughout this adjustment. The arm is horizontal, so the two linear guides are perpendicular. Thus,

$$a^2 + r^2 = a_0^2 + r_0^2 \,. \tag{30}$$

Substituting equation (29) into equation (30) yields

$$\frac{f_{CG}^2 a_0^2 r_0^2}{r^2} + r^2 = a_0^2 + r_0^2 \,, \tag{31}$$

or

$$r^4 - (a_0^2 + r_0^2) r^2 + f_{CG}^2 a_0^2 r_0^2 = 0 \,. \tag{32}$$

The roots of equation (32) were solved symbolically using the MATLAB symbolic toolbox. The equation has four roots, two of which were discarded because they were negative. The only difference between the two remaining roots was whether the distance r or a increased as f_{CG} decreased. The root that calculated r as increasing was selected because there was room alongside the arm for this displacement.

After determining the solution to equation (32), equation (29) was solved, creating symbolic expressions for both *a* and *r*. The MATLAB symbolic toolbox was also used to find the first and second derivative of both of these variables with respect to the support fraction, f_{CG}. Finally, these symbolic expressions were converted into functions that could be called from the cam synthesis code.

The simultaneous displacement cams were synthesized using the function generation method. The rotation of each idler pulley is

$$\psi_r = \frac{r - r_0}{r_p} \tag{33}$$

and

$$\psi_a = \frac{a_0 - a}{r_p}, \tag{34}$$

where r_p is the pitch radius of the idler pulley; and ψ_r and ψ_a are the rotations of the idler pulley for the cam-r and cam-a respectively. Using equation (7), the cam moment arms, h_r and h_a are

$$h_r = \frac{dr}{df_{CG}} \frac{df_{CG}}{d\theta} \tag{35}$$

and

$$h_a = \frac{da}{df_{CG}} \frac{df_{CG}}{d\theta}. \tag{36}$$

The derivatives of h_r and h_a with respect to theta are then,

$$\frac{dh_r}{d\theta} = \frac{dr}{df_{CG}} \frac{d^2 f_{CG}}{d\theta^2} + \frac{d^2 r}{df_{CG}^2} \left(\frac{df_{CG}}{d\theta} \right)^2, \tag{37}$$

and

$$\frac{dh_a}{d\theta} = \frac{da}{df_{CG}} \frac{d^2 f_{CG}}{d\theta^2} + \frac{d^2 a}{df_{CG}^2} \left(\frac{df_{CG}}{d\theta} \right)^2. \tag{38}$$

With this, the simultaneous displacement cams may be synthesized. Interestingly, the synthesis yielded infeasible cam profiles except for the special case when

$$a_0 = r_0 \, . \tag{39}$$

This is most likely because the derivatives of the support fraction with respect to each of the dimensions *a* and *r* are zero when *a* and *r* are equal, and the derivative of the support fraction with respect to elbow flexion is zero when the elbow is fully extended. Thus, this special case allows the cams to cause a non-zero displacement of the spring attachments without changing the support when the elbow is fully extended.

In designing the prototype, it was found beneficial to place an idler pulley on the carriage adjusting the attachment distance *a*. This gives the adjustment rope a 2:1 mechanical advantage. The synthesis for cam-a was adjusted for this change by simply doubling the value assigned to *a* and its derivatives. The resulting cams are shown below in Figure 26.

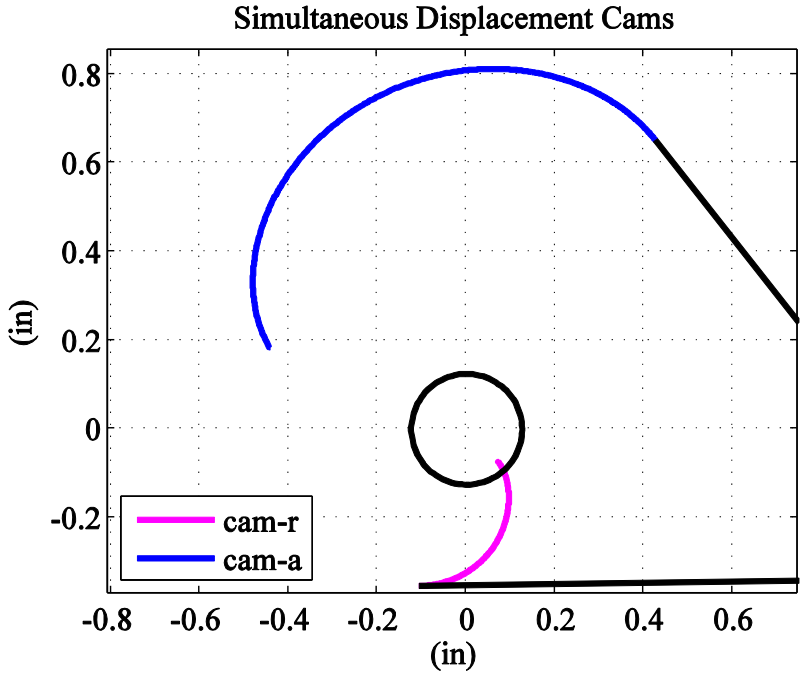

Figure 26. The simultaneous displacement cam profiles. Their ropes and the shaft about which they rotate are shown in black. The cams are shown in the orientation where the elbow is fully exentended, cam-a is fully wrapped, and cam-r is fully unwrapped. The cams would rotate clockwise as the elbow is flexed. A crossed configuration was used for cam-a.

3.4.2 Spring Cam Synthesis

The force synthesis method was used to synthesize the spring cam. The maximum rotation of the spring cam, $\theta_{s,max}$, was found using the maximum and minimum distances between the drive pulley and the idler pulley in which the arm is vertical and horizontal, respectively. Thus,

$$\theta_{s,max} = \left(a_0 + r_0 - \sqrt{a_0^2 + r_0^2}\right)\frac{2}{r_{p,s}}, \tag{40}$$

where $r_{p,s}$ is the pitch radius of the drive pulley on the spring cam. The rotation is doubled in equation (40) because of the three-pulley configuration used on the drive rope. Two lengths of rope contribute to the rotation of the drive pulley. If a spring were to be used as in a traditional gravity balancer, its spring rate, k_t, would need to be:

$$k_t = \frac{CG_0W_a}{a_0 r_0}. \tag{41}$$

However, with the pulley setup used, the spring rate in terms of the tension in the drive rope and the length of rope that unwraps for the drive pulley must be ¼ of that in equation (41). This is because two lengths of cable are exerting the force, so for a given desired force, the tension must be half. Additionally, for a given change in distance between the two pulleys, twice that distance would unwrap from the drive pulley. Thus, the spring rate simulated by the cam, k_c, is

$$k_c = \frac{1}{4}\frac{CG_0W_a}{a_0 r_0}, \tag{42}$$

and the tension in the drive rope, F_c, is

$$F_c = \theta_s r_{p,s} k_c + F_{c,0}\,, \tag{43}$$

where θ_s is the rotation of the spring cam, and

$$F_{c,0} = 2k_c\sqrt{a_0^2 + r_0^2}\,. \tag{44}$$

The work done on the simulated spring, *W*, is then

$$W = \frac{1}{2} k_c \left(\theta r_{p,s}\right)^2 + F_{c,0} \theta r_{p,s} \,, \tag{45}$$

which must be equal to the work that is by the spring connected to the cam:

$$W = \tfrac{1}{2} k x^2 + F_0 x \,, \tag{46}$$

where k is the spring rate of the physical spring; x is the stretch of the spring from its initial position with the arm horizontal; and F_0 is the tension in the spring in its initial position. Thus the stretch and force, F, in the physical spring are

$$x = \frac{-F_0 + \sqrt{F_0^2 + 2kW}}{k} \,, \tag{47}$$

and

$$F = kx + x_0 \,. \tag{48}$$

A torque balance on the spring cam and its drive pulley can then be used to determine the spring cam moment arm, h_s, defining the spring cam profile.

$$h_s = \frac{F_c r_{p,s}}{F} \,. \tag{49}$$

The resulting cam is shown in Figure 27.

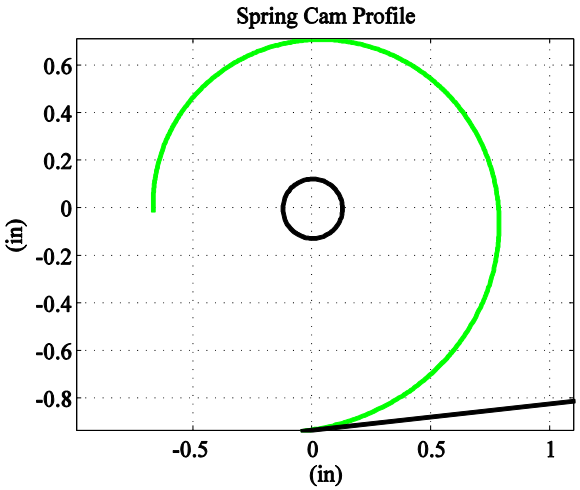

Figure 27. The spring cam profile for the simultaneous displacement prototype. The cam is shown in green, and its rope and the shaft it rotates about are shown in black

3.5 Prototype Design and Manufacturing

A prototype arm support was built to demonstrate this application of the simultaneous displacement concept. Like the series wrapping cam prototype, the base link was placed on a wall-mounted rail for vertical adjustment. However, this base link extends from the wall to a vertical, revolute joint above the user's GH. The second link wrapps around the shoulder to the next joint which passes horizontally through the user's GH. A linear guide rail for the attachment of the idler pulley of the adjustable spring mechanism is placed on this second link. The third link is placed parallel to the user's upper arm down to the elbow where it wraps 90° to the final revolute joint on the underside of the user's elbow. A linear guide rail is also placed on this link for the spring cam mechanism, and a thermoplastic cuff is fixed to this link to support the upper arm. A final link with a thermoplastic cuff is placed underneath the forearm. A pulley fixed to this link is used to drive the rotation of the simultaneous displacement cams. The completed prototype is shown below in Figure 28. A detailed CAD model of the prototype is included in the supplementary files.

(a) (b)

Figure 28. The simultaneous displacement arm support prototype in use. (a) Isometric view of the entire device. (b) Side view of the links next to the upper arm and the shoulder.

3.5.1 Simultaneous Displacement Carriage Design

For the simultaneous displacement mechanism to function, both the idler pulley and the spring cam must be allowed to move freely along their respective links. To accommodate this, each is connected to a miniature ball bearing carriage (IKO International, Santa Fe Springs, CA) and mounted to its link on a 0.27 inch (7 mm) wide linear guide rail. The ropes to the simultaneous displacement cams are attached to each carriage in a manner that aligns the rope with the rotation axis of the spring cam's drive pulley or idler pulley. Thus the force from the simultaneous displacement rope and the spring cam drive rope acts on a single point on this axis. The ball bearing carriage is placed directly underneath this pulley. This allows the carriage to behave as a three force member, requiring no moment reaction from the ball bearing carriage.

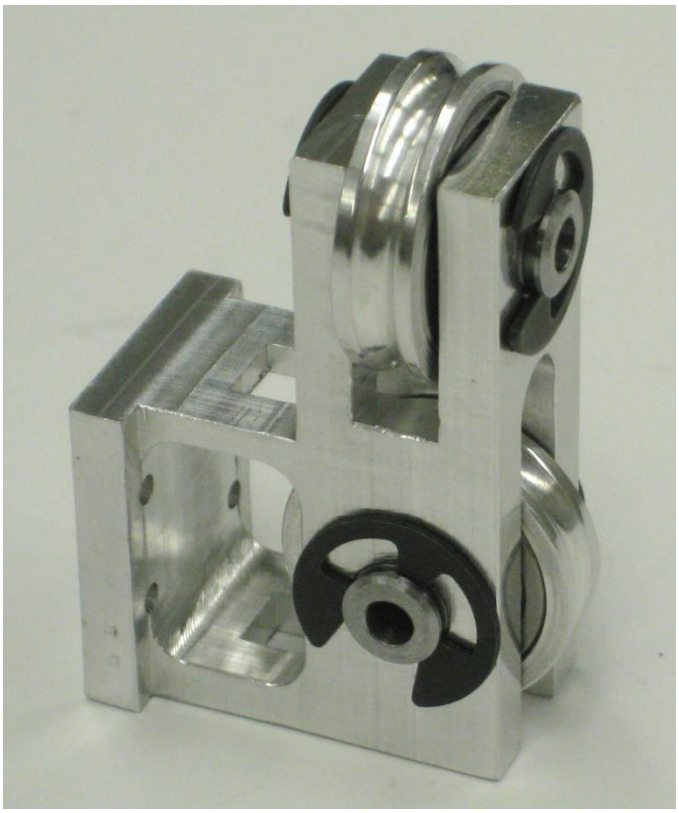

Figure 29. The carriage frame that holds the drive rope and spring cam idler pulleys. The lower pulley is the idler pulley for the spring mechanims. The upper pulley is the idler pulley for the simultaneous displacment rope. The ball bearing carriage (not shown) would be attached to the plate on the left side of the frame.

The carriage for the idler pulley is shown in Figure 29. Two slots were machined to accommodate and idler pulley for the spring mechanism rope and an idler pulley for the simultaneous displacement rope. The simultaneous displacement rope is attached to this carriage with an idler pulley for two reasons. There is more room for and better access to the adjustable cable termination on the link above, and this pulley arrangement decreases the tension in the simultaneous displacement rope by half. As this is the longest rope in the prototype, this helps to minimize stretch. This also requires that the simultaneous displacement cam be twice as large, which makes the device less sensitive to errors in the cam machining and rope width.

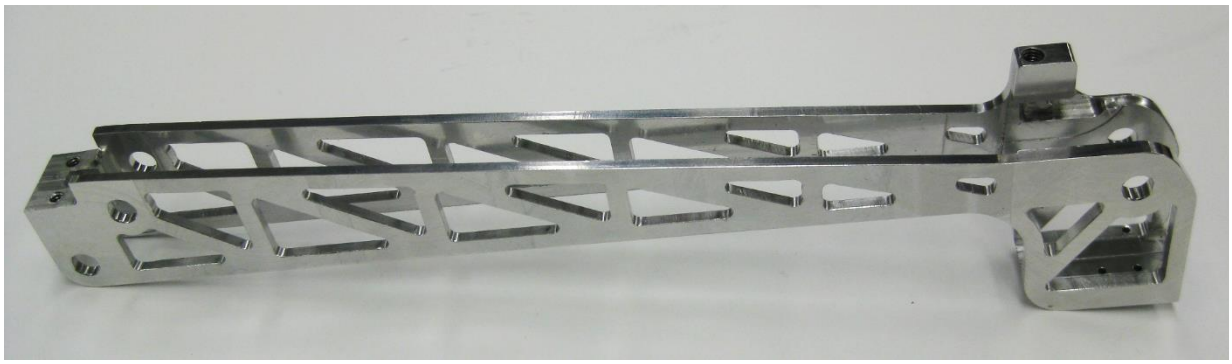

Figure 30. The carrige frame for the spring mechanism. The spring, spring cam, rope adjustment screws, and the ball bearing carriage are not shown attached to the carriage. The spring would attach via a pin through the holes at the top left, and the cam would rotate around a pin in the holes on the right. The ball bearing carriage would attach to the face connecting the two haves on the bottom right.

The frame for the spring cam is shown in Figure 30. This frame must not only hold the cam, but must also hold the spring, is very similar to the spring in the series wrapping cam prototype discussed in Section 2.4.4. Thus, this frame must have space available for the spring's full range of motion. The frame was machined as two halves in order to avoid machining a deep long channel with thin walls. Each half was machined from a 3/8-inch thick sheet of stock down to a thin plate. Protrusions were machined onto each end to space these side walls apart. A series of through pockets were machined into the frame to reduce its weight. Dowel pins were pressed into the parts to align and hold the two halves together.

The spring mechanism requires that the drive rope terminate on a pulley fixed to this frame. This "pulley" was machined directly onto the frame using a convex-radius end mill. A pathway for the rope was also machined into the side, leading to the adjustment screw. These features are shown in Figure 31.

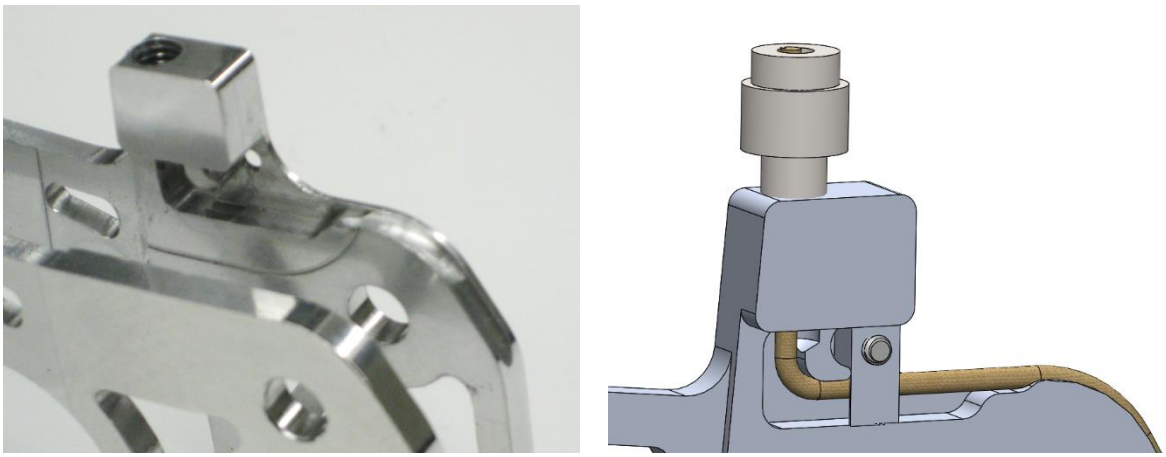

(a) (b)

Figure 31. The drive rope routing through the spring cam carriage frame. (a) A close up of the actual part. The radiused grove for the rope to wrap over the corner can be seen on the top right edge. (b) A SolidWorks screenshot of the rope routing with the adjustment screw and the rope included. At the bottom center, the rope is covered up by a small piece bolted onto the frame. This piece is in place to ensure that the rope remains aligned with the radiused grove on the edge of the frame.

3.5.2 Link Design

Many of the links require space for the spring and cam mechanisms inside them, especially those supporting the linear guide rails for the simultaneous displacement mechanism. Because of this, these links were machined as deep channels. Two of these links must wrap around a joint but also require this channel to face along the upper arm. In order to meet these requirements with a reasonably machinable design, these sections of the links were machined as two pieces. These pieces slip into each other and are screwed together. The various channel-shaped pieces are shown in Figure 32.

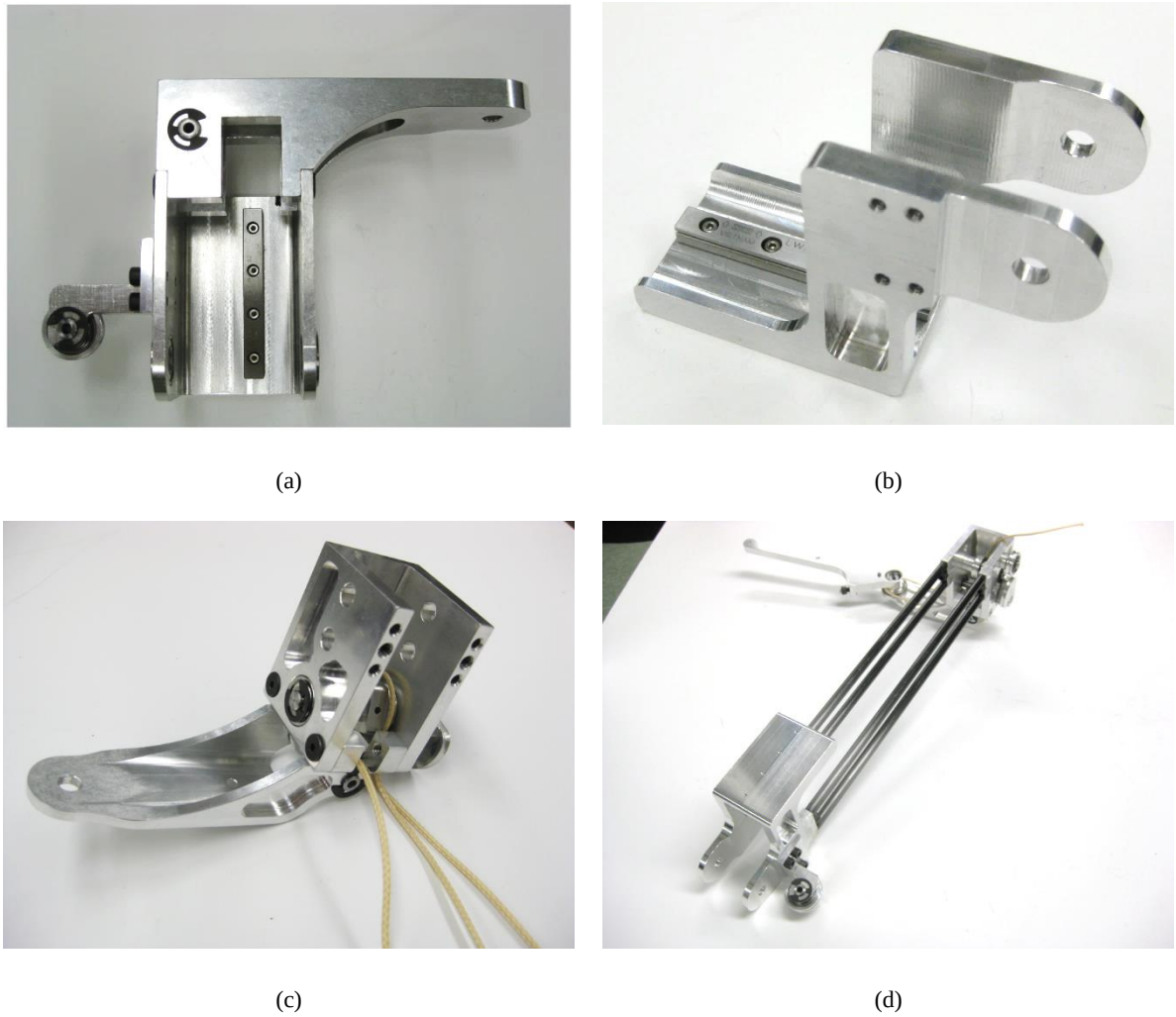

(a) (b)

(c) (d)

Figure 32. The various links designed to allow clearance for internal mechanisms. (a) The link placed next to the shoulder. The guide rail would be oriented vertically. Attached to this rail would be the idler pulley for the drive rope of the spring cam. (b) The most proximal piece of the upper arm link. The guide rail would be oriented parallel to the centerline of the upper arm. Attached to this rail would be the spring cam mechanism. (c) The most distal piece of the upper arm link. This piece wraps underneath the elbow. (d) The two ends of the upper arm link from (b) and (c) connected by the carbon fiber rod structure. The forearm link is also shown attached in this picture.

The spring mechanism also requires clearance through the horizontal rotation axis. In order to accommodate this, two pins are used to support the upper arm link. This structure is shown in Figure 33.

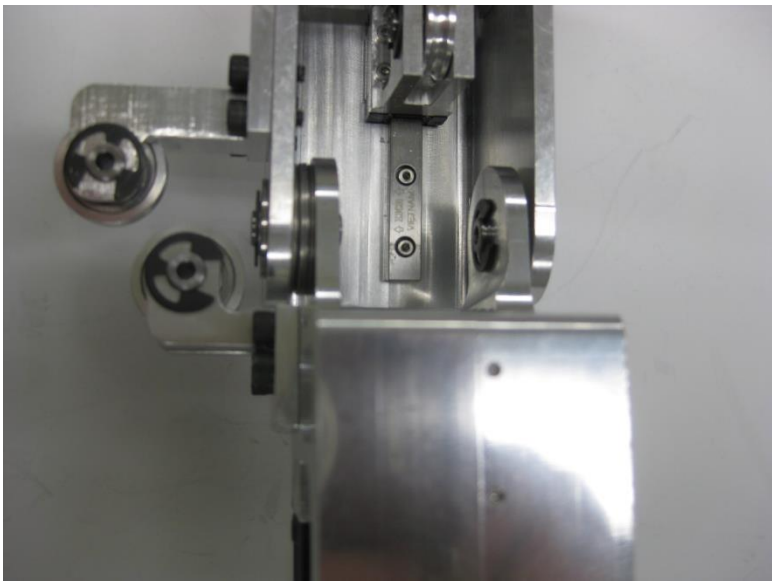

Figure 33. The horizontal joint next to the shoulder with two pins used to provide clearance for the drive rope of the spring cam.

For the link along the upper arm, it was necessary to create a long structure with clearance for the spring mechanism inside. In the interest of saving weight, this structure was made from pultruded carbon fiber tubes. Aluminum terminations were machined to hold two carbon fiber rods. Dowell pins 1/8-inch in diameter were pressed into the terminations so they can be precisely located on the proximal and distal frames of the upper arm link, and a through hole was drilled through the center so that the termination can held onto the frame by a screw. Cylindrical projections were CNC milled onto the other end of the terminations such that the carbon fiber rods could slip onto these projections. The carbon fiber rods were then epoxied to the aluminum terminations. The surface was sanded radially with 120 grit sandpaper, prepped with Alumiprep and Alodine, and epoxied with Loctite 120 HP according to the recommendations of [37]. The carbon fiber assembly is shown in Figure 34.

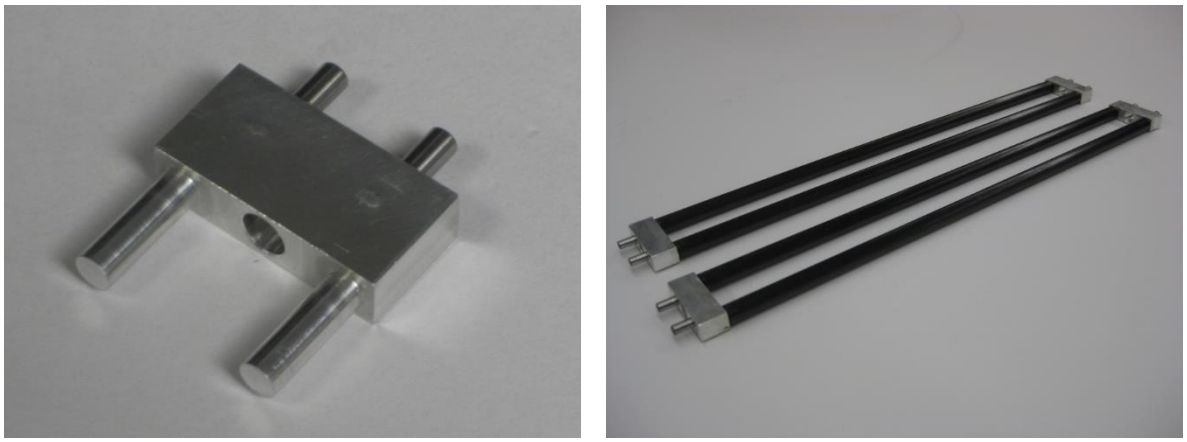

(a) (b)

Figure 34. The carbon fiber structure used for the length of the upper arm link. (a) An aluminum end piece to which the carbon fiber rods were epoxied. The protrosuions (bottom left) were machined directly onto the part. They were inserted into and epoxied to the carbon fiber tubes. The dowel pins for attachement to the rest of the link frame are visible on the top right. The through hole in the center allows the assembly to be bolted to the rest of the frame. (b) The carbon fiber rods and their end terrminals assembled and epoxied.

3.5.3 Simultaneous Displacement Cam Placement

In order to maintain a low-profile elbow joint, the simultaneous displacement cams are placed on the side of the elbow, where space on the frame is available, instead of underneath the elbow. An antagonistic pulley system, shown in Figure 35, is used to couple the rotation of these cams to elbow flexion. A pulley with terminations for two cables is fixed to the shaft supporting the cams in order to drive their rotation. These cables are routed straight down to idler pulleys which directs them under the elbow to the final link. There, they wrapp around a pulley machined onto the final link and then terminate on two adjustment screws. The use of two antagonistic cables ensures that the elbow can rotate the cams both directions when the arm is horizontal.

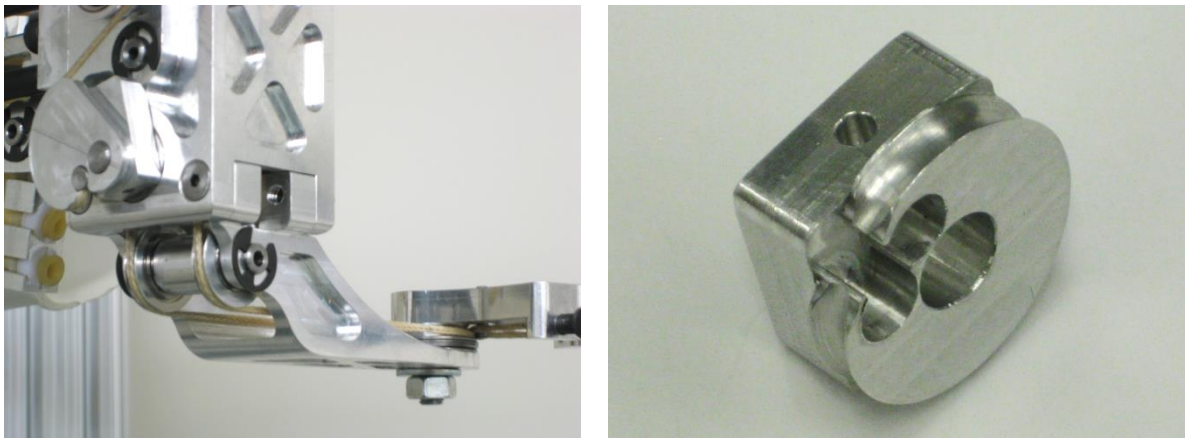

(a) (b)

Figure 35. The antagonistic drive ropes coupling elbow flexion with the simultaneous desplacement cams. (a) The rope routing from the simultaneous displacement cams to the forearm link. The forearm link is shown on the right. On the bottom left are the two pulleys that route the two cables up to the simultaneous displacement cams' drive pulley. This drive pulley is hiddin within the frame of the upper arm link. (b) The drive pulley for the simultaneous displacement cams.

3.5.4 Simultaneous Displacement Rope Routing

Both of the ropes actuated by the simultaneous displacement cams must be routed through the prototype to their respective carriages. Both ropes first pass over an idler pulley in order to ensure that the cable aligns with the subsequent pulley or carriage. After this pulley, the rope actuating the upper-arm carriage connects directly to the carriage. The rope actuating the vertical carriage, however, must be routed past the shoulder joint without being affected by shoulder elevation. In order to accomplish this, two pulleys are placed directly next to the shoulder joint on both the link parallel to the arm and the link next to the shoulder. These pulleys are placed such that the short section of rope between them is collinear with the joint axis. Thus, when the arm is raised or lowered, the rope does not wrap around any pulley but simply twists along this section. The rope is then routed to a pulley above the vertical carriage so the rope passes straight down to the carriage pulley and then straight back up to its adjustment screw. This arrangement can be seen in Figure 36.

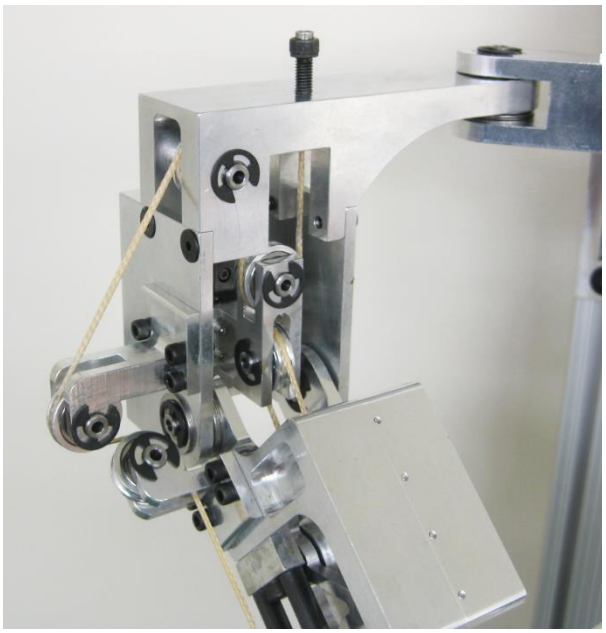

Figure 36. The rope routing through the shoulder joint. Two pulleys (bottom left) are placed next to the horizontal shoulder joint creating a short length of rope collinear with the joint axis. The rope is routed up to a pulley (top left) above the verical carriage (center), then down to a pulley on the vertical carriage, and then back up to the adjustment screw (top center).

3.5.5 Cam and Pulley Design and Manufacturing

As with the previous prototype, the cams were machined on a CNC mill; however, for this prototype, a convex radius end mill was used to cut round grooves for the rope.

The simultaneous displacement cams must be fixed to each other, so that they rotate together. However, one cam must be placed outside of the frame, so they could not be manufactured from a single piece of stock. Instead, the cams and their drive pulley are fixed to the support shaft with dowel pins. In order to ensure proper alignment, both of the simultaneous displacement cams and their drive pulley were CNC milled with a rectangular protrusion on one side. This rectangle was placed in the same orientation on all cams providing a flat surface to reference and to drill radially through the hole for the support shaft. The support shaft was machined with holes to position each cam relative to the others. Both the holes in the shaft and the cams were drilled and reamed to a 3/32 inch slip fit. The cams and shaft were assembled within the frame, then 3/32 inch dowel pins were pushed into the cams and the shaft with slip

fit retaining compound (Loctite, Düsseldorf, Germany) to hold the pins in place. The simultaneous displacement cams, drive pulley, and shaft are shown in Figure 37.

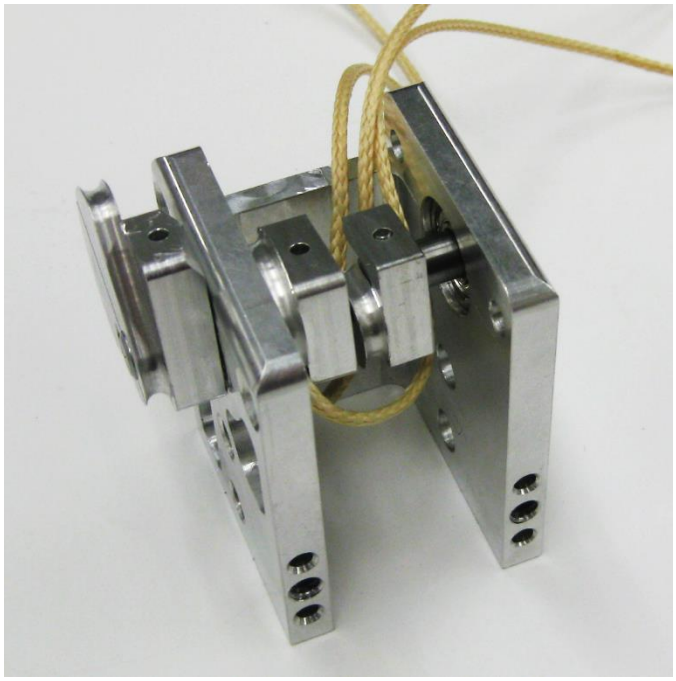

Figure 37. The simultanous displacement cams assembled on their support shaft. The cam actuating the vertical carriage is on the left; the drive pulley in the middle; and the cam actuating the upper arm carriage is on the right. The holes for the dowel pins can be seen on the top of the flats of the cams. This assembly is part of the upper arm frame near the elbow.

The profile of the cam that actuates the upper arm carriage passes very close to the center of its axis of rotation. In order to allow clearance for this cam, a slot was machined halfway through the supporting shaft. The cam was then machined with a slot through its side. This slot allows the cam to be slipped onto the shaft from its side. This slot must be tangent to the end point of the cam curve. Thus, it was this feature that was used to define the orientation of the rectangular protrusion on the simultaneous displacement cams and their drive pulley. The shaft and this cam are shown in Figure 38.

(a) (b)

Figure 38. The cam and support shaft machined to allow rope clearance near the rotation axis. (a) The simultaneous displacment cams' support shaft. (b) The cam that actuates the upper arm carriage.

Figure 39. The spring cam. The drive pulley is visible on the top face of the cam. A standoff the same width as the drive pulley exists on the other side of the cam, but it is not visible in this picture.

The spring cam was manufactured on a tooling plate in a similar manner as the series cam was. Because the cable to the cam connects to the spring, which has very little clearance between it and the frame, the cam surface must be centered between the sides of the frame. The

pulley for the drive cable is machined directly onto the spring cam. Flanged bearings are pressed into both sides of the spring cam with extended races protruding slightly from each side, supporting the cam against the slight axial load that the drive cable places on it. The spring cam is shown in Figure 39.

Custom idler pulleys were also machined using a CNC lathe. These pulleys aredesigned with a ¾-inch pitch diameter, which is nearly the smallest possible pulley diameter that would fit around the outside diameter of the bearings selected for this high load.

3.5.6 Rope Assembly and Adjustment

As with the previous prototype, potted terminations are used to attach the ropes to their cams and adjustment screws. However, space limitations required that the diameter of the terminations be reduced to 3/16-inch. Adjustment screws were created by drilling through 10-32 socket cap screws.

A variety of jigs were 3D printed in order to facilitate the cutting of the ropes to the correct lengths and the subsequent adjustment of the rope lengths with the adjustment screws. These jigs hold the various joints, cams, and carriages in their home position. With all these components held in a specific orientation relative to each other, ropes could be pulled taught and cut to length. When adjusting the rope length with the adjustment screw, some of the adjustments must be made with the jig removed. When the jig is able to fit onto its mating assembly, then its associated ropes are adjusted correctly. Some of the jigs only constrain the assembly in one direction, so the rope may be adjusted until it makes contact with the jig. Two of these jigs are shown in Figure 40.

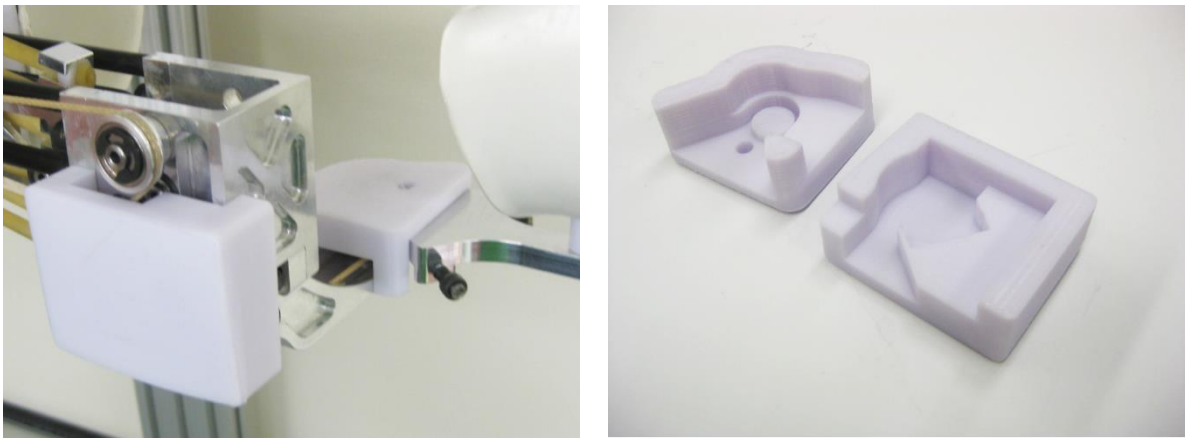

(a) (b)

Figure 40. The 3D printed jigs used for adjustment of the antagonistic drive rope of the simultaneous displacement cams. (a) The jigs in use for adjustment. (b) The inside of the jigs. The top left jig constrains the elbow joint to be fully extended. The bottom right jig fixes the simultaneous displacement cams in their correct orientation.

All ropes were potted on the end that attaches to their cam or pulley first. Then, they were threaded through the device and finally through their adjustment screw. With the adjustment screw all the way in and the device fixed in place by the jigs, the rope was pulled tight and marked at the end of the termination. The jigs were then removed so that the rope could be pulled out of the termination far enough to pot the terminations. The spring cam rope was potted first because it was easiest to handle with the carriage removed from the prototype. The remaining ropes were potted in the following order: the antagonistic drive ropes for the simultaneous displacement cams first, the ropes that connect directly to the simultaneous displacement cams second, and the drive rope of the spring cam last. This allowed subsequent ropes to utilize those potted earlier, but with the jigs, this was not entirely necessary.

When adjusting the prototype with the full spring load on the ropes, it was found that the adjustment screws are not long enough to completely adjust some of the mechanisms on the prototype. Due to time limitations, a solution to this problem was not pursued, and the device was tested with this error in its adjustment present.

3.6 Device Testing

3.6.1 Qualitative Assessment

The simultaneous displacement prototype was tested qualitatively by using it to support an arm. This test showed that the general gravity balancing behavior of the device is as intended. When the arm is horizontal, very little effort is necessary to flex or extend the elbow. When lowering the arm, the support provided to the shoulder joint is noticeably lower with the elbow flexed than with the elbow extended. The support torque provided to the shoulder also decreases appropriately as the arm is lowered. Finally, the prototype provides assistance in elbow flexion when the upper arm is lowered.

Some significant shortcomings were also clearly evident in the prototype. Most notably, the elbow joint exhibits a very high amount of friction, especially when the arm is lowered and the elbow is extended. Additionally, the support provided to the elbow when the upper arm is lowered seems to be too high in a region around 45° elbow flexion. The combination of this friction and support profile error make it very difficult to fully extend the elbow when the arm was down. This problem is compounded by the inadequacies of the interface between the arm and prototype. The cuffs are unable to adequately constrain the prototype to move with the arm. When attempting to extend the elbow against the support, the device tends to push the user's elbow out of alignment. This misalignment also tends to cause an undesired rotation about the vertical axis through the shoulder. This is also due in part to the prototype being in a singular configuration when the upper arm is straight down.

In addition to these shortcomings, some other mechanical issues were observed. The carbon fiber structure, while strong enough to handle the bending and compression loading, is very flexible in torsion. This causes the spring carriage to collide with and rub on the frame that

holds the simultaneous displacement cams. Another issue observed is that the drive pulley of the spring cam interferes with the drive rope when the elbow is flexed and the arm is horizontal. This is due to an error in the design of the cable attachment to the drive pulley. The spring cam was redesigned to address this problem, but time was not available to machine a second spring cam. The error introduced by this interference should have only a minor impact on the device behavior in a small region of its range of motion. Finally, the drive pulley of the simultaneous displacement cams was found to rub against frame next to it. This could be fixed by removing the simultaneous displacement cams and machining a thin layer off of their support frame to provide clearance.

3.6.2 Quantitative Torque Measurement

Quantitative measurements of the torque profiles generated by the prototype were taken using similar load cell and potentiometer setups as that used to test the series cam prototype. Torque profiles for both the shoulder joint and the elbow joint were measured. Because these two joints were coupled to each other, multiple torque profiles for each joint were measured with the other joint fixed in different positions using jigs made from laser cut plywood. The two test setups are shown in Figure 41.

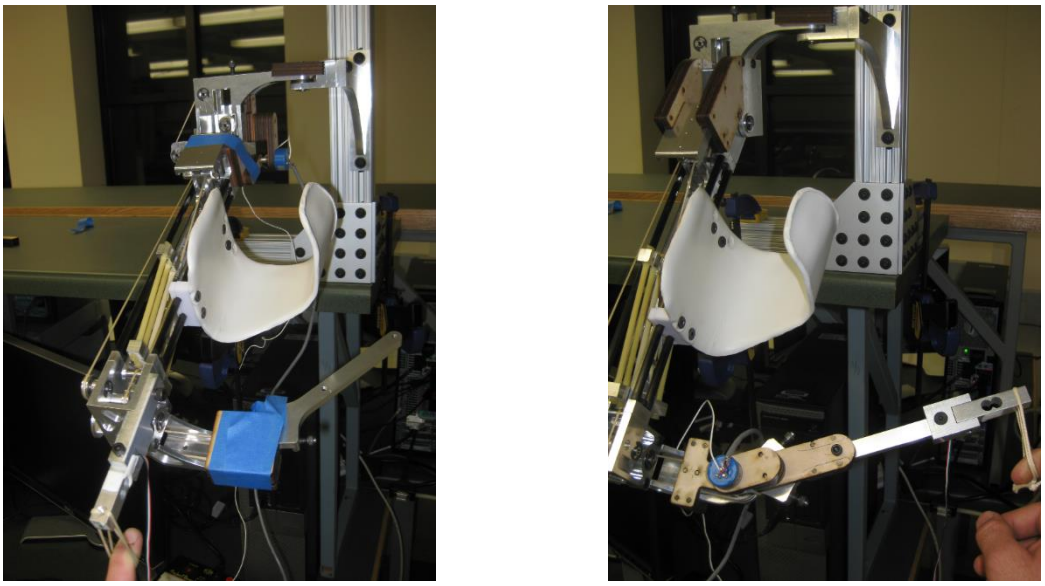

(a) (b)

Figure 41. The torque measurment test setups. (a) The test setup for measuring the torque about the shoulder joint. The potentiometer is connected at the shoulder joint (top center), and the load cell is connected to the distal end of the upper arm link (bottom left). The elbow joint (bottom right) is fixed at 135° flexion by the laser-cut jig which is wrapped in blue tape. (b) The test setup for measuring the torque about the elbow joint. The potentiometer is connected to the elbow joint (bottom left) and the load cell is connected to the distal end of the forearm link (bottom right). The shoulder joint is fixed at 45° below horizontal by the laser-cut jigs (top left).

The results from the testing of the shoulder joint are shown in Figure 42. The shoulder joint behaves basically as designed. As the arm is lowered, the torque decreases sinusoidally to zero when the arm is down. Likewise, the support is appropriately scaled down as the elbow is flexed. However, multiple errors, similar to those in the series cam prototype, are present in this prototype. First, support torque does not reach its maximum until the upper arm is about 10° below horizontal. This is likely due to errors in spring length or rope adjustment. This error is compounded with greater elbow flexion, because the spring cam rotates less, requiring the upper arm to be lowered further before reaching the configuration in which it behaves properly. Second, the prototype consistently provides too little support. As the elbow is flexed, the percentage of this error appears to increase. This error also likely results from errors in the adjustment of the spring cam drive rope and the spring rope as well as errors in the spring assembly/characterization. As expected, hysteresis is present in the device.

The results from the testing of the elbow joint are shown in Figure 43. As with the shoulder joint, the elbow joint roughly exhibits the desired behavior. The elbow joint produced a sinusoidal support torque when the upper arm is down, and this support torque decreases to around zero when the arm is horizontal. The behavior of the elbow joint, however, exhibits much greater error than that of the shoulder joint. Most notably, the friction in this joint is very severe. The cause of this friction is unclear. The rubbing of the simultaneous displacement drive pulley is likely responsible for much of this friction. It is possible that the large number of pulleys and the large wrap angle necessary to route the ropes for the simultaneous displacement mechanism are responsible. Many of the bearings in these pulleys are under very high loads. Additionally, the rubbing of fibers within the rope as it bends around pulleys would introduce friction. Finally, the bearing design in the elbow joint may not be appropriate to handle the complex loading it experiences.

The torque profile also appears to be shifted in the direction of elbow extension. This is why the device provides too much support to the elbow around 45° elbow flexion. The reason for this error is unclear, but it is likely due to stretch in the rope or errors in the rope adjustment. Likely, this error arises from the antagonistic ropes coupling the elbow joint to the simultaneous displacement cams. These ropes exhibit visible elongation as they are loaded. This elongation would cause the simultaneous displacement cams to rotate prematurely, creating the shift in the torque profile. The possibility that an error exists in the cam synthesis was also considered, but a careful evaluation of the synthesis did not reveal any error.

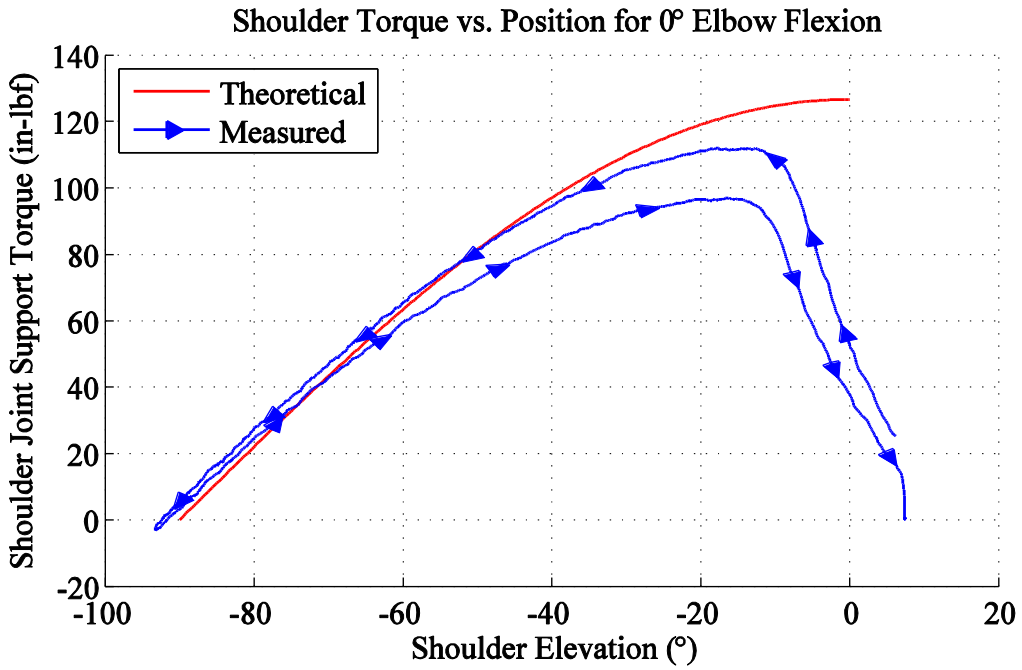

(a)

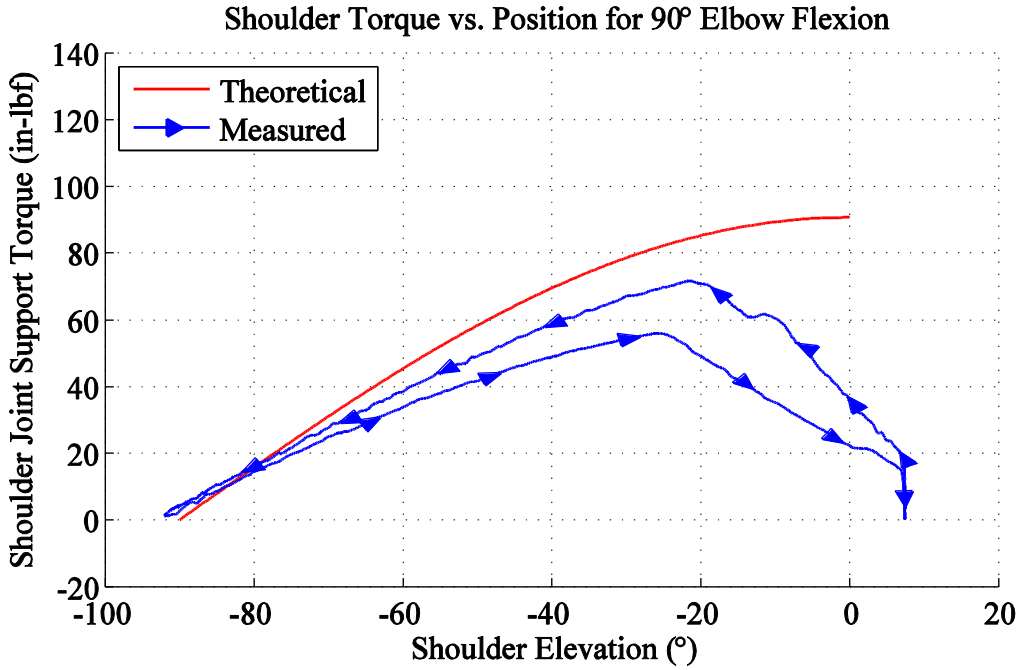

(b)

Figure 42. The measured torque/position behavior of the shoulder joint. The arrows on the measured line indicate the direction of travelt. (a) The torque profile at the shoulder when the elbow is at 0° flexion (fully extended). (b) The torque profile at the shoulder when the elbow is flexed 90°.

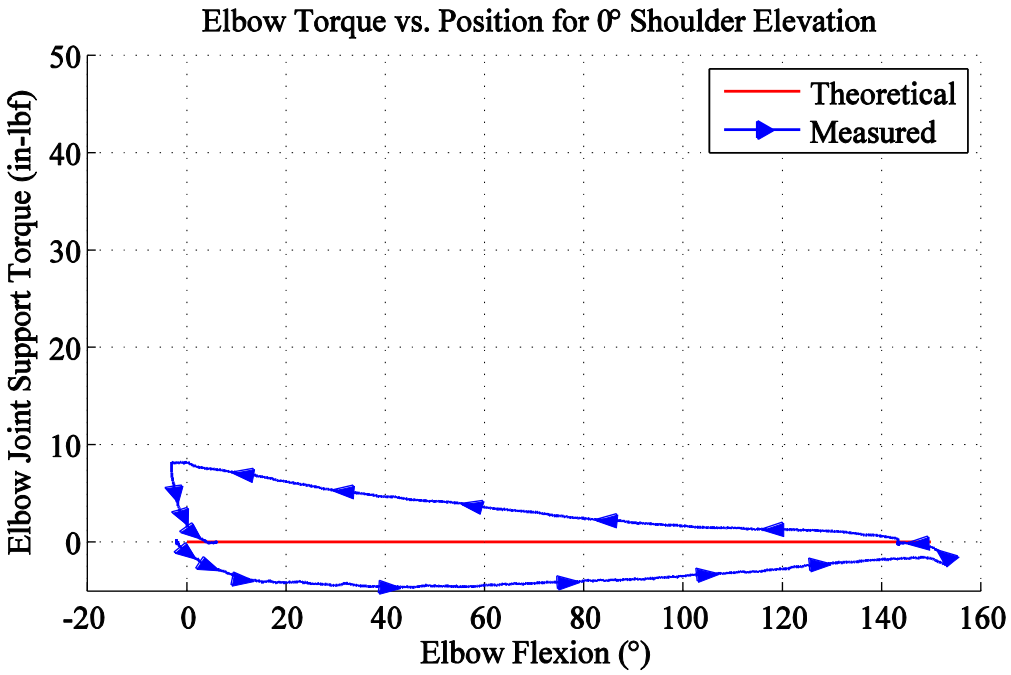

(a)

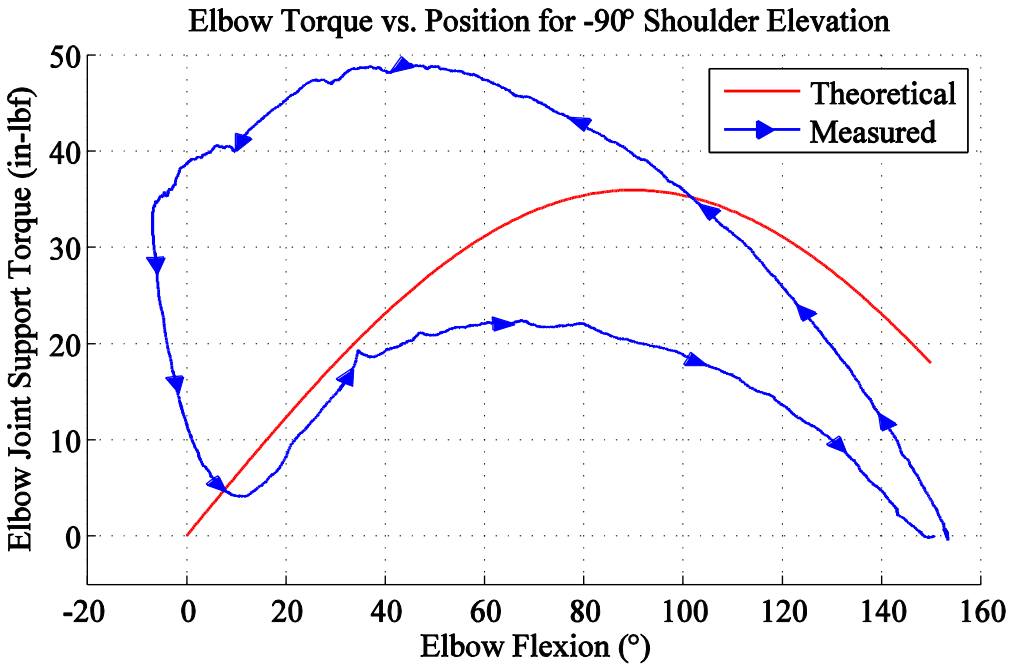

(b)

Figure 43. The measured torque/positon behavior of the elbow joint. The arrows on the measured line indicte the direction of travel. (a) The torque profile at the elbow joint for 0° shoulder elevation (arm horizontal). (b)The torque profile at the elbow for -90° shoulder elevation (arm fully lowered).

3.7 Discussion

The application of the simultaneous displacement concept to couple elbow flexion with shoulder torque has the potential to reduce the profile of an arm support device. This allows the entire support mechanism to remain on the upper arm supporting link. Additionally, the entire forearm supporting link remains hidden underneath the elbow. The mechanism does not require a parallelogram linkage along the upper arm, which makes it simpler to enclose.

The prototype presented in this chapter successfully demonstrates the feasibility of using this mechanism in a wearable arm support. The device exhibits all the intended behavior. The simultaneous displacement mechanism very effectively reduces the support provided to the shoulder joint as the elbow is flexed. Additionally, this adjustment requires little effort when the arm is horizontal, as intended. Finally, the device provides assistance in elbow flexion when the arm is lowered.

However, the device behavior also exhibits some significant errors. The error in the support torque provided to the shoulder is similar to that in the series wrapping cam. As with the series wrapping cam, improvements in spring design and manufacturing as well as cable adjustment could dramatically improve this behavior.

The errors in the behavior of the elbow joint are much more significant. The design and adjustment of the antagonistic ropes driving the simultaneous displacement cams should be improved to reduce the elongation and backlash. Increasing the tension in both of the ropes might help. Additionally, the ropes could be adjusted so that the cams are in the correct position when the system is under highest tension (arm down) rather than when the device is horizontal. The friction in the elbow joint is very severe. An analysis of the root cause of this friction is necessary to determine whether reduction of friction in this mechanism is possible. Preventing

the drive pulley from rubbing and improving the joint design of the elbow may address this issue. However, if this friction is predominantly from the pulleys, little may be done to reduce the friction to an acceptable level. To reduce this, minimizing the total wrap angle of the cable would be necessary. If the bending of woven fibers in the ropes is a cause of friction, using an unwoven belt would minimize this type of friction.

For an early proof of concept, this prototype is reasonably low profile, but future iterations of the design should seek to further reduce its size. Many parts of the prototype, such as the elbow joint, could be made lower profile with little effort. However, a number of aspects to this prototype will make further reduction in size difficult. The rope routing through the shoulder is especially high profile because the rope is directed directly out from the arm. A planar mechanism could be implemented to reduce the size of this mechanism at the cost of further complexity. This rope should be routed in a manner that allows its cam to be placed inside the structure of the upper arm link. The number of parts and assemblies that move within each other would also make it difficult to reduce the thickness of the link supporting the upper arm. The use of a linear guide rail next to the shoulder and the rope routing above it limits the extent to which the link next to the shoulder may be wrapped around the shoulder. Finally, the high forces in this mechanism place a limit on the size of components such as bearings and guide rails.

The prototype exhibited some shortcomings that were not related specifically to the simultaneous displacement mechanism. These issues should not be too difficult to address in future prototypes. The structure of the upper arm link should be redesigned to be much less flexible in torsion. A composite shell structure would serve the dual purpose of enclosing the device and providing a very rigid structure.

4 Conclusion

4.1 Summary

The work presented in this thesis was conducted in the interest of improving the wearability of arm support devices for people who have suffered a stroke. Specifically, novel gravity balance mechanisms were sought in order to make a lower profile arm support mechanism. Two different mechanisms featuring wrapping cams were designed. Prototype arm supports with these mechanisms were constructed and tested.

The first mechanism was called the series wrapping cam. This mechanism uses a wrapping cam to stretch a spring, storing the arm's gravitational potential energy as it is lowered. This cam is connected to another cam, called the drive cam, which defines the rotation of the cams in relation to shoulder elevation. The use of two cams allows a small spring with a relatively low initial tension to be used without requiring an unreasonably large cam.

A prototype arm support was built using the series wrapping cam mechanism. The prototype has one supported DOF at the shoulder and a passive DOF at the elbow. Testing showed that the series wrapping cam mechanism creates roughly the correct shoulder joint torque profile with some error due to inaccurate cable adjustment, cable stretch, inaccurate spring assembly/characterization, and friction. The prototype was not designed to respond to elbow flexion. Using the arm support showed that this is an unacceptable limitation.

The second mechanism was designed to address this limitation. It uses a variation of the traditional gravity balancer to support the upper arm. The balancer is placed on two linear guide rails, allowing the support at the shoulder to be reduced in response to elbow flexion by two wrapping cams. These cams utilize the simultaneous displacement method for energy free adjustment [23], allowing the elbow to be flexed without effort when the arm is horizontal.

Additionally, when the upper arm is lowered, the mechanism supplies assistance in raising the forearm against gravity. The benefit of this mechanism is that none of the support mechanism extends beyond the elbow, potentially making it lower profile.

A prototype was constructed using the simultaneous displacement mechanism. It has 3 degrees of freedom with a passive, vertical joint through the shoulder, a supported, horizontal joint though the shoulder, and a supported joint through the elbow coupled to the shoulder joint support mechanism. As with the series cam prototype, testing showed that the prototype behaves generally as it was designed to with errors due to inaccuracies in assembly and adjustment, cable stretch, and friction. The elbow joint particularly exhibits a very high amount of friction. Two parts were found to be rubbing, which could be the cause of much of this friction. The large number of pulleys with high forces utilized by this prototype, however, may also be a source of friction.

Building these prototypes presented some unique design challenges. Steel wire rope could not be used for the wrapping cams due to bending fatigue on the small radii of the cams. Vectran synthetic fiber rope was used instead, and a compact rope termination was constructed using resin potted terminals. A small, lightweight spring was constructed from latex tubing by placing nylon balls in the ends and then placing the ends in plates with hemispherical cups. This spring was significantly shorter than a steel coil spring capable of similar deflections would be. A lightweight structure was made using four pultruded carbon fiber rods, but this design is not recommended for this application due to its inadequate torsional stiffness.

4.2 Future Work

Because the series wrapping cam could not be coupled to elbow flexion, any advantage of the series wrapping cam over the mechanism used in WREX is not evident. Thus, applying

the series wrapping cam in any orthoses with multiple supported degrees of freedom in series is not recommended. However, the series wrapping cam may still be valuable in single degree of freedom orthoses that require a force or torque profile that a simple spring cannot create. For example, the series wrapping cam could be used in a hand orthosis to create a similar torque profile as that created by HandSOME [29] but without the 4-bar mechanisms.

The simultaneous displacement mechanism has the potential to create a lower profile, wearable arm support. However, more work is required to create a successful, wearable arm support. As discussed in Section 2.6, significant improvement to the mechanical design of the mechanism is necessary. Most importantly, friction in the elbow joint and its associated support mechanisms must be reduced. Additionally, rope stretch must be accounted for through better adjustment, and possibly through considering cable elongation in the cam synthesis. The spring must be more accurately manufactured and characterized. Some potential improvements to the spring design were discussed in Section 2.6. Finally, the size of the mechanism should be minimized as much as possible.

Adjustability of the support provided by the arm support would be a useful feature that was not fully realized in this work. The current design only allows the support to be reduced to ⅔ and ⅓ of full support. Users need to be able to fine-tune the support to match their individual needs on a day to day basis. The simplest method to do this would be to use multiple elastic bands that can be added or removed as is done on the WREX [18]. However, a mechanism that could allow continuous adjustment without opening the device and adding or removing parts would be ideal. This is non-trivial, especially when using cams, because the spring force must be scaled. Perhaps the initial values of the spring attachment locations, a_0 and r_0, could be

adjusted. However, this would require the simultaneous displacement mechanism to adjust the distances *a* and *r* as percentages of their initial positions.

For simplicity, this prototype restricted the shoulder joint to two degrees of freedom. This still allows the hand to be placed in any location, but this additional degree of freedom would give the user the freedom to place their elbow in a range of orientations for a given hand placement. This limitation will make some movements feel less natural, and interactions with objects, such as tables will be more difficult. Adding a joint along the upper arm may be possible, but coupling this joint to the other two joints would be significantly more complicated. One solution might involve tilting the vertical guide rail. When the arm undergoes external rotation, the center of gravity of the arm rises above the center line of the upper arm. The gravity balance mechanism, however responds only to the orientation of the upper arm, and requires the center of gravity to lie on this centerline. Tilting the rail backwards during external rotation would compensate for this. Considering the complexity of this mechanism, a user study would be valuable to evaluate whether having only three degrees of freedom is sufficient to meet the needs of the user.

This thesis focused on the gravity balance mechanism in the arm support. Other aspects to the arm support design must be considered to make it wearable. Comfortable attachment of the device to the user's body poses a difficult challenge critical to the success of the device. A frame – probably a backpack – must be added to attach the device to the user's torso. This frame would need to maintain the first joint in alignment with the shoulder. It would also need to comfortably transfer the weight of the arm and the device as well as the support torque to the user's torso. Preferably, this would be accomplished with minimal restriction of trunk mobility. Additionally, the device must be attached to the arm. This attachment must be firm enough to

keep the device in alignment with both the elbow and shoulder joints without causing excessive pressure and especially shear stress on the user's skin. Additionally, the visibility of these attachments should be considered.

Finally, with a refined design completed, a user study must be conducted in order to evaluate its effectiveness as a rehabilitation device. This would be necessary first to see if people are willing to wear, and continue to wear, the orthosis. Second, it must be determined whether the orthosis encourages use of the affected limb in activities of daily living. Finally, the study should evaluate the long-term effects of wearing the orthosis. It is important to ensure that the device does not lead to a decrease in functionality of the affected limb. This might occur if the gravity support causes muscle atrophy. If long-term use of the device leads to improvement in the functionality of the affected limb, the orthosis may become a valuable tool for stroke rehabilitation.

Works Cited

[1] B. H. Dobkin, "Rehabilitation after Stroke," *The New England journal of medicine*, vol. 352, no. 16, pp. 1677-1684, 2005.

[2] D. Mozaffarian *et al.*, "Executive Summary: Heart Disease and Stroke Statistics-2016 Update: A Report From the American Heart Association," *Circulation*, vol. 133, no. 4, p. 447, 2016.

[3] C. E. Han, M. A. Arbib, and N. Schweighofer, "Stroke Rehabilitation Reaches a Threshold," *PLoS Comput Biol*, vol. 4, no. 8, p. e1000133, 2008.

[4] A. Kunkel *et al.*, "Constraint-induced movement therapy for motor recovery in chronic stroke patients," *Archives of physical medicine and rehabilitation*, vol. 80, no. 6, pp. 624-628, 1999.

[5] C. Patten, J. Lexell, and H. Brown, "Weakness and strength training in persons with poststroke hemiplegia: Rationale, method, and efficacy," in *J. Rehabil. Res. Dev.* vol. 41, no. 3, 2004, pp. 293-312.

[6] J. P. A. Dewald, P. S. Pope, J. D. Given, T. S. Buchanan, and W. Z. Rymer, "Abnormal muscle coactivation patterns during isometric torque generation at the elbow and shoulder in hemiparetic subjects," *Brain*, vol. 118, no. 2, pp. 495-510, 1995.

[7] T. M. Sukal, M. D. Ellis, and J. P. A. Dewald, "Shoulder abduction-induced reductions in reaching work area following hemiparetic stroke: neuroscientific implications," *Experimental Brain Research*, vol. 183, no. 2, pp. 215-223, 2007.

[8] J. L. Herder, *Energy-free Systems. Theory, conception and design of statically*. 2001.

[9] J. L. Herder, "Development of a statically balanced arm support: ARMON," in *9th International Conference on Rehabilitation Robotics, 2005. ICORR 2005.*, 2005, pp. 281-286.

[10] (2016, August 11). *SaeboMAS | Saebo*. Available: http://www.saebo.com/saebomas/

[11] (2016, August 11). *Elevating MAS w/ Forearm Support - Jaeco Orthopedic*. Available: http://jaecoorthopedic.com/products/products/Elevating-MAS-w%7B47%7D-Forearm-Support-.html

[12] (2016, August 11). *Edero from Armon - Armon Products BV*. Available: http://www.armonproducts.com/products/edero/

[13] (2016, August 11). *Darwing - Focal Meditech*. Available: http://www.darwing.nl/home-en.html

[14] G. Kramer, G. R. B. Romer, and H. J. A. Stuyt, "Design of a Dynamic Arm Support (DAS) for gravity compensation," in *Rehabilitation Robotics, 2007. ICORR 2007. IEEE 10th International Conference on*, 2007, pp. 1042-1048.

[15] B. Mastenbroek, E. de Haan, M. van den Berg, and J. Herder, "Development of a Mobile Arm Support (Armon): Design Evolution and Preliminary User Experience," in *Rehabilitation Robotics, 2007. ICORR 2007. IEEE 10th International Conference on*, 2007, pp. 1114-1120.

[16] (2016, August 11). *Gowing | Focal Meditech*. Available: http://www.focalmeditech.nl/en/content/gowing

[17] (2007). *Setup Instructions for WREX*. Available: http://www.jaecoorthopedic.com/Manuals/WREXManual5.28.2008Complete.pdf

[18] T. Rahman, W. Sample, S. Jayakumar, and M. M. King, "Passive exoskeletons for assisting limb movement," *Journal of rehabilitation research and development*, vol. 43, no. 5, p. 583, 2006.

[19] (2016, August 11). *The JAECO WREX - Wilimington Robotic Exoskeleton, WREX MultiLink Arm*. Available: http://jaecoorthopedic.com/products/products/WREX%3A-Wilmington-Robotic-EXoskeleton-Arm.html

[20] A. Dunning and J. Herder, "A review of assistive devices for arm balancing," in *Rehabilitation Robotics (ICORR), 2013 IEEE International Conference on*, 2013, pp. 1-6: IEEE.

[21] P. Tidwell, "Wrapping cam mechanisms," C. Reinholtz, Ed., ed: ProQuest Dissertations Publishing, 1995, p. 69 p.

[22] P. H. Tidwell, N. Bandukwala, S. G. Dhande, C. F. Reinholtz, and G. Webb, "Synthesis of wrapping cams," *Journal of Mechanical Design*, vol. 116, no. 2, pp. 634-638, 1994.

[23] W. D. van Dorsser, R. Barents, B. M. Wisse, and J. L. Herder, "Gravity-Balanced Arm Support With Energy-Free Adjustment," *Journal of Medical Devices*, vol. 1, no. 2, pp. 151-158, 2007.

[24] (2016, August 8). *Design Info - Guidelines For Cable Assembly Selection*. Available: http://www.savacable.com/pages/applic_02.html

[25] (2016, August 8). *Kuraray Vectran™ Properties*. Available: http://www.vectranfiber.com/properties/

[26] (2016, August 15). *Vectrus - Single Braided Rope & Single Braid Rope - Industrial Rope | Yale Cordage*. Available: http://www.yalecordage.com/industrial-rope/single-braided-ropes/vectrus.html

[27] P. B. Stimson, "A Review of Methods for Termination of Synthetic- Fiber Ropes," Coast Guard Research and Development Center., Groton., CT, no. CGR/DC-36/75, 1975.

[28] (December 18, 2014). *Primeline Industries: Download Center and Online Tools*. Available: http://www.primelineindustries.com/tools.html

[29] E. B. Brokaw, R. J. Holley, and P. S. Lum, "Hand Spring Operated Movement Enhancer (HandSOME) device for hand rehabilitation after stroke," in *2010 Annual International Conference of the IEEE Engineering in Medicine and Biology*, 2010, pp. 5867-5870.

[30] M. Kilic, Y. Yazicioglu, and D. F. Kurtulus, "Synthesis of a torsional spring mechanism with mechanically adjustable stiffness using wrapping cams," *Mechanism and Machine Theory*, vol. 57, pp. 27-39, 2012.

[31] R. Barents, M. Schenk, W. D. van Dorsser, B. M. Wisse, and J. L. Herder, "Spring-to-Spring Balancing as Energy-Free Adjustment Method in Gravity Equilibrators," *Journal of Mechanical Design*, vol. 133, no. 6, p. 061010, 2011.

[32] B. M. Wisse, W. D. v. Dorsser, R. Barents, and J. L. Herder, "Energy-Free Adjustment of Gravity Equilibrators Using the Virtual Spring Concept," in *2007 IEEE 10th International Conference on Rehabilitation Robotics*, 2007, pp. 742-750.

[33] D. A. Winter, *Biomechanics and motor control of human movement*. John Wiley & Sons, 2009.

[34] R. F. Chandler, C. E. Clauser, J. T. McConville, H. M. Reynolds, and J. W. Young, "Investigation of inertial properties of the human body," DTIC Document1975.

[35] B. M. Nigg and W. Herzog, *Biomechanics of the musculo-skeletal system*. John Wiley & Sons, 2007.

[36] Anthropometry and Biomechanics | NASA.gov [Online]. Available: https://msis.jsc.nasa.gov/sections/section03.htm

[37] A. C. Çobi, "Design of a carbon fiber suspension system for FSAE applications," 2012.

Appendix – MATLAB Code

Series Wrapping Cam Synthesis

The following code was used to synthesize the two cam profiles for the series wrapping cam mechanism. The code generates a list of 500 points for each cam surface and saves the data as a .txt file which is compatible for importing as a curve in SolidWorks.

```
%Series Wrapping Cam Synthesis
%Arm support research
%Jeremiah Schroeder
%6/11/15

clear all; close all; clc

%Constants
W=10;                %Arm Weight (lbf)
L=12;                %Arm length (in)
rp=1;                %Pitch radius of fixed shoulder pulley (in)
cdd=2.75;            %Center distance to shoulder pulley (in)
cds=7.75;            %Center distance to spring attachment (in)
n=500;               %Number of data points
thetamax=255*pi/180;%Maximum cam rotation (rad)
psimax=79*pi/180;    %Maximum arm rotation (rad)
t=1/16;              %Cable thickness (in)
ns=6;                %Number of springs
k=ns*1.7;            %Spring Stiffness (lbf/in)
F0=ns*.5;            %Spring intercept (lbf)
x0=2;                %Initial displacemetn of spring (in)

%Arbitrary constants used for generation of cam rotation function
c1=pi/5;
c2=2;
c3=thetamax/((psimax+c1)^(1/c2)-c1^(1/c2));

%Cam Synthesis

%psi = rotation of the pulley = rotation of the users arm
psi=linspace(0,psimax,n);

fileID1=fopen('WrappingCam1.txt','wt');
fileID2=fopen('WrappingCam2.txt','wt');

for i=1:1:n

    %Drive Cam - Specified displacement

    %Rotation of cam
    %Arbitrary function to control the rotation of the cam
    %
    %The goal is to produce cam with an increasing radius as the arm goes
down
```

```
    %giving the cam a beneficial mechanical advantage while the arm is up
    %and still turning as much as possible through the range of motion
    %
    %Should start at zero with a non-infinite, non-zero, positive,
    %decreasing slope
    theta(i)=c3*((psi(i)+c1)^(1/c2)-c1^(1/c2));

    %Derivitive of pulley rotation wrt cam rotation
    dp_dt(i)=c2/c3*(theta(i)/c3+c1^(1/c2))^(c2-1);

    %Second derivitive of pulley rotation wrt cam rotation
    d2p_dt2(i)=c2*(c2-1)/c3^2*(theta(i)/c3+c1^(1/c2))^(c2-2);

    %Cam moment arm                                        (Eq. 5.30, pg. 47)
    hd(i)=rp*dp_dt(i);

    %Derivitive of moment arm wrt cam rotation             (Eq. 5.31, pg. 47)
    dhd_dt(i)=rp*d2p_dt2(i);

    %Derivitive of moment arm angle, phi wrt cam rotation(Eq. 5.17, pg. 45)
    dphid_dt(i)=-1/sqrt(cdd^2-(hd(i)+rp)^2)*dhd_dt(i);

    %moment arm angle (crossed assembly)                   (Eq. 5.19, pg. 45)
    phid(i)=acos((hd(i)+rp)/cdd);

    %free length of cable                                  (Eq. 5.15, pg. 45)
    qd(i)=cdd*sin(phid(i))/(1+dphid_dt(i));

    %Vector to cam surface                                 (Eq. 5.18, pg. 45)
    xd(i)=cdd*cos(theta(i)+pi)+(-t/2-
rp)*cos(theta(i)+phid(i)+pi)+qd(i)*cos(theta(i)+phid(i)+3*pi/2);
    yd(i)=cdd*sin(theta(i)+pi)+(-t/2-
rp)*sin(theta(i)+phid(i)+pi)+qd(i)*sin(theta(i)+phid(i)+3*pi/2);

    xyz=[xd(i); yd(i); 0];

    fprintf(fileID1,'%f\t %f\t %f \n',xyz);


    %Spring Camm

    %This Cam must meet two requirements:
    %1 - It must produce the proper spring deflection to store the arms
    %energy
    %2 - It mus have the appropriate moment arm to match this spring
    %tension to the necessary torque to balnce the arm

    %Torque on cam found through force balance on cable between pulley and
    %first cam
    T(i)=W*L*cos(psi(i))/rp*hd(i);

    %Spring displacement (Conservation of Energy)
    x(i)=(-F0+sqrt(F0^2+2*k*(W*L*sin(psi(i))+1/2*k*x0^2+F0*x0)))/k;

    %Spring Force
    F(i)=k*x(i)+F0;
```

```
    %Torque balance between cam 1 and cam 2
    hs(i)=T(i)/F(i);

    %moment arm angle                                    (Eq. 5.16, pg. 45)
    phis(i)=acos(hs(i)/cds);

    %Deriritive of moment arm wrt cam rotation - using chain rule
    dx_dt(i)=(F0^2+2*k*(W*L*sin(psi(i))+1/2*k*x0^2+F0*x0))^(-
1/2)*(W*L*cos(psi(i)))*dp_dt(i);
    dF_dt(i)=k*dx_dt(i);
    dT_dt(i)=-W*L*sin(psi(i))*dp_dt(i)^2+W*L*cos(psi(i))*d2p_dt2(i);

    dhs_dt(i)=(F(i)*dT_dt(i)-T(i)*dF_dt(i))/F(i)^2;

    %Derivitive of moment arm angle wrt cam rotation     (Eq. 5.17, pg. 45)
    dphis_dt(i)=-1/sqrt(cds^2-hs(i)^2)*dhs_dt(i);

    %free length of cable                                (Eq. 5.15, pg. 45)
    qs(i)=cds*sin(phis(i))/(1-dphis_dt(i));

    %Vector to cam surface                               (Eq. 5.18, pg. 45)
    xs(i)=cds*cos(theta(i))-(t/2)*cos(theta(i)-phis(i))+qs(i)*cos(theta(i)-
phis(i)-pi/2);
    ys(i)=cds*sin(theta(i))-(t/2)*sin(theta(i)-phis(i))+qs(i)*sin(theta(i)-
phis(i)-pi/2);


    xyz=[xs(i); ys(i); 0];

    fprintf(fileID2,'%f\t %f\t %f \n',xyz);

end

fclose(fileID1);
fclose(fileID2);

%plotting
%create lines for ropes
lined=[xd(1) yd(1)];
lines=[xs(1) ys(1)];
dy_dxd=(yd(2)-yd(1))/(xd(2)-xd(1));
lined(2,:)=[xd(1)-1 yd(1)-dy_dxd]
lines(2,:)=[cds 0];

%create circle for shaft
thc=linspace(0,2*pi,100);
circle=.125*exp(1i*thc);

figure
plot(xd,yd,'r-',xs,ys,'g-','LineWidth',2)
axis equal
axis square
grid on
hold on
xlim manual
ylim manual
```

```
plot(lined(:,1),lined(:,2),'-k',lines(:,1),lines(:,2),'-k','LineWidth',2)
plot(circle,'k','LineWidth',2)
legend('Drive Cam','Spring Cam','Location','SW')
title('Cam Profiles')
xlabel('(in)')
ylabel('(in)')
```

Simultaneous Displacement Cam Synthesis

The following code was used to synthesize the two cams for the simultaneous displacement mechanism and their associated spring cam. The code generates a list of 500 points for each cam surface and saves the data as a .txt file which is compatible for importing as a curve in SolidWorks.

```
%Jeremiah Schroeder
%Arm Support Research
%Simultaneous Displacement Elbow Adjustment
%9/28/15

clear all; close all; clc

n=500;                    %Number of evaluation points
a0=1.5;                   %Initial vertical attachment location (in)
r0=1.5;                     %Initail horizontal attachment location (in)
rp_e=3/8;                %Pitch radius of pulley next to elbow cams (in)
theta_max=pi*5/6;         %Elbow range of motion (rad)
theta=linspace(0.001,theta_max,n);
cd_e=.875;                   %center distance between elbow cams and pulley
(in)
cd_e2=1.45;
t=1/16;                   %cable thickness (in)
rp_s=.375;                 %pitch radius of the pulley driving the spring cam
(in)
cd_s=8.5;                   %distance from spring attachment to center of
spring cam (in)

%Arm  Parameters
W=1*200;                  %Body weight (lbf)

%Segment fraction of body weight
PW_u=.0286;               %Upper Arm
PW_f=.0173;               %Forearm
PW_h=.00691;               %Hand

%Device weight
W_dev_f=0.32;             %forearem
W_dev_u=1.34;             %upper arm

%Device CG
CG_dev_f=3.60;               %forearm
CG_dev_u=7.41;               %upper arm

%Segment Weight (lbf)
W_ua=PW_u*W;
W_fa=PW_f*W;
W_h=PW_h*W;
W_f=W_fa+W_h+W_dev_f;            %hand plus forearm plus device
```

```
W_u=W_ua+W_dev_u;               %upper arm plus device
W_a=W_f+W_ua+W_dev_u;           %Total Arm

%Fraction of limb segment length to center of gravity
PL_u=.475;
PL_f=.417;
PL_h=.470;

%Segment length (in)
L_u=12;
L_f=11;
L_h=7.5;

%Center of gravity (in)
CG_ua=PL_u*L_u;
CG_fa=PL_f*L_f;
CG_h=PL_h*L_h;
CG_f=(W_fa*CG_fa+W_h*(CG_h+L_f)+W_dev_f*CG_dev_f)/W_f;
CG_u=(W_ua*CG_ua+W_dev_u*CG_dev_u)/W_u;
CG_0=(W_u*CG_u+W_f*(L_u+CG_f))/W_a;

%Arm center of gravity (in)
CG=(W_u*CG_u+W_f*(L_u+cos(theta)*CG_f))/W_a;

%%
%Synthesis of cams that move attachment locations a and r with elbow
%rotation
%cam_1 adjusts position r
%cam_2 adjusts position a

%Fraction of maximum arm support required as forearm is moved in
f_cg=CG/CG_0;
% and its derivative with respect to theta (1/rad)
dfcg_dth=-W_f/W_a*CG_f/CG_0*sin(theta);
d2fcg_dth2=-W_f/W_a*CG_f/CG_0*cos(theta);

%Attachment positions r and a and derivatives with respect to support
%fraction c (in)
[r,dr_dfcg,d2r_dfcg2]=r_f(f_cg,a0,r0);
[a,da_dfcg,d2a_dfcg2]=a_f(f_cg,a0,r0);

%update a with idler pulley on carriage
a=2*a;
da_dfcg=2*da_dfcg;
d2a_dfcg2=2*d2a_dfcg2;
a0=2*a0;

%Rotation of pulleys nearest to elbow cams (rad)
psi_r=(r-r0)/rp_e;
psi_a=(a0-a)/rp_e;

%Cam moment arm (in)
h_r=dr_dfcg.*dfcg_dth;          %(Equation 5.30)
h_a=-da_dfcg.*dfcg_dth;
```

```
%Derivatives of moment arm with respect to elbow rotation theta (in/rad)
dh_dth_r=dr_dfcg.*d2fcg_dth2+d2r_dfcg2.*dfcg_dth.^2;
dh_dth_a=-da_dfcg.*d2fcg_dth2-d2a_dfcg2.*dfcg_dth.^2;

%Angle between centerline and moment arm (rad)
% phi_r=acos((h_r+rp_e)/cd_e); %(Crossed, Equation 5.19)
phi_a=acos((h_a+rp_e)/cd_e2);
phi_r=acos((h_r-rp_e)/cd_e); %(Un-crossed, Equation 5.16)
% phi_a=acos((h_a-rp_e)/cd_e2);

%Derivative of angle between centerline and moment arm (rad/rad)
% dphi_dth_r=-1./sqrt(cd_e^2-(h_r+rp_e).^2).*dh_dth_r; %(Crossed, Equation
5.20)
dphi_dth_a=-1./sqrt(cd_e2^2-(h_a+rp_e).^2).*dh_dth_a;
dphi_dth_r=-1./sqrt(cd_e^2-(h_r-rp_e).^2).*dh_dth_r; %(Un-Crossed, Equation
5.17)
% dphi_dth_a=-1./sqrt(cd_e2^2-(h_a-rp_e).^2).*dh_dth_a;

%Length of cable (in)
q_r=cd_e*sin(phi_r)./(1-dphi_dth_r);    %(Equation 5.15)
q_a=cd_e2*sin(phi_a)./(1+dphi_dth_a);

%Vector to cam surface  (in)
%(Crossed: Equation 5.18, modified)
% P_r=cd_e*exp(1i*theta)-(t/2+rp_e)*exp(1i*(theta-
phi_1))+q_1.*exp(1i*(theta-phi_r-pi/2));
P_a=cd_e2*exp(1i*theta)-
(t/2+rp_e)*exp(1i*(theta+phi_a))+q_a.*exp(1i*(theta+phi_a+pi/2));
%(Un-Crossed: Equation 5.10)
P_r=cd_e*exp(1i*theta)+(-t/2+rp_e)*exp(1i*(theta-
phi_r))+q_r.*exp(1i*(theta-phi_r-pi/2));
% P_r=cd_e2*exp(1i*theta)+(-
t/2+rp_e)*exp(1i*(theta+phi_2))+q_2.*exp(1i*(theta+phi_a+pi/2));

plot(P_r,'m','LineWidth',2)
hold on
plot(P_a,'b','LineWidth',2)
axis equal
grid on
xl=xlim;
yl=ylim;

delta_r=(P_r(2)-P_r(1));
delta_a=(P_a(2)-P_a(1));
line_r=[P_r(1) P_r(1)+delta_r*1000];
line_a=[P_a(1) P_a(1)+delta_a*-1000];
plot(line_r,'k','LineWidth',2)
plot(line_a,'k','LineWidth',2)
axis([xl*1.05 yl*1.05])

title('Simultaneous Displacement Cams')
xlabel('(in)')
ylabel('(in)')
legend('cam-r','cam-a','Location','SW')
```

```
thp=linspace(0,2*pi,100);
shaft=.125*exp(1i*thp);
plot(shaft,'k','LineWidth',2)


%%
%Synthsis of a cam to simulate higher rate spring

%Rotation of spring cam (rad)
a0=1/2*a0;

theta_s_max=(a0+r0-sqrt(a0^2+r0^2))*2/rp_s;
theta_s=linspace(0,theta_s_max,n);

%Simulated spring characteristics
k_s=CG_0*W_a/(a0*r0)/4;     %Simulated spring rate (lbf/in)
F0_s=k_s*2*sqrt(a0^2+r0^2);   %Simulated inital spring force (lbf)

%Actual spring characteritics
ns=6;                %Number of tubes
L=1.4;                 %Tube length (in)
Fmax=9;           %Force in 1 tube at 400% elongation (lbf)
Fmin=3.9;           %Force in 1 tube at 100% elongation (lbf)
x0=.5;              %Initial deflection beyond L (in)
rp_is=0;          %Radius of idler pulley for spring cam (in)

k=ns*(Fmax-Fmin)/(3*L); %Spring rate of combined tubes (lbf/in)
F0=ns*Fmin+k*x0;        %Initial force in spring (lbf)

%Force in simulated spring (lbf)
F_sim=theta_s*rp_s*k_s+F0_s;

%Work done on simulated spring (lbf*in)
W=1/2*k_s*(theta_s*rp_s).^2+F0_s*(theta_s*rp_s);

%Displacement of actual spring (in)
x=(-F0+sqrt(F0^2+2*k*W))/k;

%Force in spring (lbf)
F=k*x+F0;

%Cam moment arm (in)
h_s=F_sim*rp_s./F;

%Derivative of moment arm with respect to theta
dF_sim_dth=rp_s*k_s; %derivative of simulated spring force (lbf/rad)
dW_dth=k_s*theta_s*rp_s^2+F0_s*rp_s;
dx_dth=(F0^2+2*k*W).^(-1/2).*dW_dth;
dF_dth=k*dx_dth; %derivative of actual spring force (lbf/rad)
dh_dth_s=(F.*dF_sim_dth*rp_s-F_sim*rp_s.*dF_dth)./F.^2; %derivative of
moment arm (in/rad)

%Angle between centerline and moment arm (rad)
```

```
phi_s=acos((h_s+rp_is)/cd_s); %(Crossed, Equation 5.19)
% phi_s=acos((h_s-rp_is)/cd_s); %(Un-crossed, Equation 5.16)

%Derivative of angle between centerline and moment arm (rad/rad)
dphi_dth_s=-1./sqrt(cd_s^2-(h_s+rp_is).^2).*dh_dth_s; %(Crossed, Equation
5.20)
% dphi_dth_s=-1./sqrt(cd_s^2-(h_s-rp_is).^2).*dh_dth_s; %(Un-Crossed,
Equation 5.17)


%Length of cable (in)
q_s=cd_s*sin(phi_s)./(1-dphi_dth_s);    %(Equation 5 from journal paper)

%Vector to cam surface  (in)
%(Crossed: Equation 3, from journal paper)
P_s=cd_s*exp(1i*theta_s)-0*(t/2+rp_is)*exp(1i*(theta_s-
phi_s))+q_s.*exp(1i*(theta_s-phi_s-pi/2));
% (Un-Crossed: Equation 5.10)
% P_s=cd_s*exp(1i*theta_s)+(-t/2+rp_is)*exp(1i*(theta_s-
phi_s))+q_s.*exp(1i*(theta_s-phi_s-pi/2));


figure
plot(P_s,'-g','LineWidth',2)
grid on
hold on
axis equal
xl=xlim;
yl=ylim;
line_s=[P_s(1) cd_s];
plot(line_s,'-k','LineWidth',2)
plot(shaft,'-k','LineWidth',2)
axis([xl yl])
title('Spring Cam Profile')
xlabel('(in)')
ylabel('(in)')

%%
%Save data
xyz1=[real(P_r)' imag(P_r)' zeros(length(P_r),1)];
xyz2=[real(P_a)' imag(P_a)' zeros(length(P_a),1)];
xyzs=[real(P_s)' imag(P_s)' zeros(length(P_s),1)];

fileID1=fopen('WrappingCam1.txt','wt');
fileID2=fopen('WrappingCam2.txt','wt');
fileIDs=fopen('WrappingCams.txt','wt');

for i=1:1:n

fprintf(fileID1,'%f\t %f\t %f \n',xyz1(i,:));
fprintf(fileID2,'%f\t %f\t %f \n',xyz2(i,:));
fprintf(fileIDs,'%f\t %f\t %f \n',xyzs(i,:));

end
```

```
fclose(fileID1);
fclose(fileID2);
fclose(fileIDs);

%Convert distance a back to its original value
a=a/2;
```